THE IMPORTANCE OF LIFETIME OF MICELLES IN RELATION TO VARIOUS TECHNOLOGICAL PROCESSES

BY

SEONG-GEUN OH

A DISSERTATION PRESENTED TO THE GRADUATE SCHOOL
OF THE UNIVERSITY OF FLORIDA IN PARTIAL FULFILLMENT
OF THE REQUIREMENTS FOR THE DEGREE OF
DOCTOR OF PHILOSOPHY

UNIVERSITY OF FLORIDA

1993

To

My Parents, Wife and Sons

ACKNOWLEDGEMENTS

I would like to express my sincere appreciation to Professor Dinesh O. Shah, chairman of my supervisory committee, for his kind guidance and encouragement during my Ph.D. program. Thanks are due to Professor Ranga Narayanan, Chang-Won Park, Gerald B. Westermann-Clark and Brij M. Moudgil for their valuable time and advice in serving as members of the Supervisory Committee.

I wish to thank all my colleagues in the Chemical Engineering Department for their help and cooperation. C.P. Singh, Y.K. Rao, P. Kumar, V. Pillai, P. Huibers and all other friends in our research group, I will always remember the times and endeavors that we shared to achieve our goal. I wish them all the best of luck and bright futures. I would also like to acknowledge the financial support of the Alcoa Foundation and the Proctor & Gamble Company for this research.

Finally, I owe my gratitude to my family for their love and encouragement throughout these years.

TABLE OF CONTENTS

LIST OF TABLES

LIST OF FIGURES

Abstract of Dissertation Presented to the Graduate School
of the University of Florida in Partial Fulfillment of the
Requirements for the Degree of Doctor of Philosophy

THE IMPORTANCE OF LIFETIME OF MICELLES IN RELATION TO VARIOUS TECHNOLOGICAL PROCESSES

By

Seong-Geun Oh

December 1993

Chairperson: Dinesh O. Shah
Major Department: Chemical Engineering

The lifetime (or stability) of micelles has been of great academic interest in order to understand dynamic behavior of micelles in solution. However, the relevance of micellar lifetime to various technological processes such as foaming, bubble dynamics, emulsification, wetting, detergency and rate of solubilization of oil in micellar solutions has never been explored. In this study, systematic research has been carried out to delineate the role of micellar lifetime on the dynamic processes in micellar solutions. The pressure-jump technique was used to measure the relaxation time (τ_2) of SDS (sodium dodecyl sulfate) micelles, which is related to the

micellar lifetime. The slow relaxation time (τ_2) of SDS was maximum at 200 mM concentration at 25°C, indicating that the most stable micelles are formed at this concentration. During dynamic processes such as foaming, emulsification, bubble generation and textile wetting in micellar solution, the interface between two phases is expanding very rapidly. The rate of diffusion of surfactant monomers from the bulk to the interface influences the dynamic interfacial tension. This dynamic interfacial tension determines the characteristics of dynamic processes. The relatively unstable micelles can augment significantly the diffusion rate of monomers in determining the dynamic interfacial tension. The most stable micelles at a 200 mM concentration of SDS resulted in the least foaming, the largest bubble size, the minimum frequency of bubble formation, the longest wetting time of textile, the largest emulsion droplet size in the mixture of hexadecane/SDS solutions and the most rapid solubilization of oil into micellar solutions. A mathematical simulation on the diffusion rate of monomers in micellar solutions showed that the diffusion rate from bulk to the interface is determined by the micellar lifetime rather than by the total surfactant concentration. In addition, the effect of tetraalkylammonium ions on the stability of SDS foam and the esterification reaction of stearic acid by lipozyme in foam have been studied.

CHAPTER 1
DYNAMIC PROPERTIES OF MICELLAR SOLUTIONS

1.1 Theory

Micelles are in a dynamic equilibrium state with monomers in solution above the critical micelle concentration.[1] Namely, micelles are dissociated into monomers and monomers are associated into micelles continuously. Micelles are formed in the solution due to the existence of a hydrophobic group in the surfactant molecules and the van der Waal's attraction force between the hydrocarbon chains of surfactant molecules; they are dissociated by the thermal motion of surfactant molecules in the micelles.[2] In the words of Winsor, "Micelles are of a statistical character, and it is important to guard against a general picture of micelles as persistent entities having well-defined geometrical shapes".[3] The multiequilibrium, stepwise association process of micelle formation can be described as[4]

$$A_1 + A_1 = A_2$$

$$A_1 + A_2 = A_3$$

$$A_1 + A_3 = A_4$$

.

$$A_1 + A_{n-1} = A_n$$

where A_1 denotes the surfactant monomer and A_n represents the micellar aggregate with aggregation number n. These micellar kinetics have been studied by stopped-flow,[5] temperature-jump,[6] pressure-jump[7] and ultrasonic absorption[8,9] methods since Aniansson[10] developed a theoretical model about the kinetics of micellization. There are two relaxation processes. The first one is the fast relaxation process with relaxation time τ_1 (in the range of 10^{-8} to 10^{-3} second) which is associated with the fast exchange of monomers between micelles and bulk aqueous phase. This process is due to the exchange of the surfactant molecules between the micelles and the bulk. It is related to the residence time of the surfactant molecules in the micelles. The second relaxation time, characterized by the relaxation time τ_2 (in the range of 10^{-3} to 10 seconds), is associated with the reaction of micellar breakdown-formation (Figure 1-1).[11] τ_2 is related to the micellar lifetime and the average micellar lifetime is given by the following expression.[12,13]

$$\frac{1}{\tau_2} = \frac{n^2}{A_1 R}\left(1 + \frac{\sigma^2}{n} a\right)^{-1} \qquad (1.1)$$

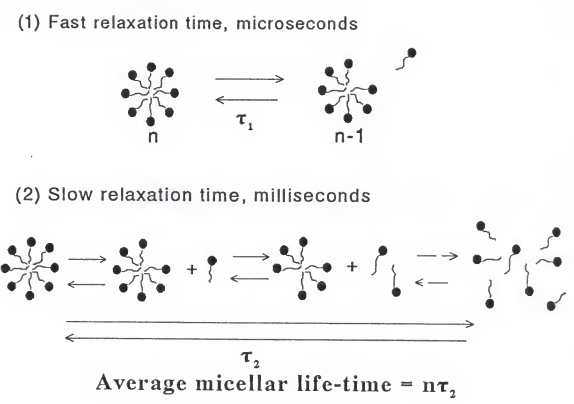

Figure 1-1. A schematic illustration of mechanisms for the two micellar relaxation times in surfactant solution.

$$T(m) = \tau_2 \frac{na}{1 + \frac{\sigma^2}{n} a} \tag{1.2}$$

where T(m) is the average micellar-life time, τ_2 is the second relaxation time, n is the aggregation number, σ is the distribution width of the distribution curve of micellar aggregates and $a = (A_{tot} - A_1)/A_1$, where A_{tot} and A_1 are the total surfactant concentration and mean monomer concentration, respectively, as shown in the distribution curve of micellar size (Figure 1-2), and R is given by[12]

$$R = \sum_{s=s_1+1}^{s_2} 1/(k_s^{-1} A_s) \tag{1.3}$$

where s is the aggregation number of a particular aggregate, k_s^{-1} is the dissociation rate constant of this aggregate and A_s is the equilibrium concentration of aggregates with an aggregation number of s. The dependence of τ_2 on ionic strength, concentration and temperature can be interpreted in terms of their effects on R.[14] When the concentration of surfactant is much greater than the critical micelle concentration (CMC), σ^2/n is of the order of one and a $[= (A_{tot} - A_1)/A_1]$ is much

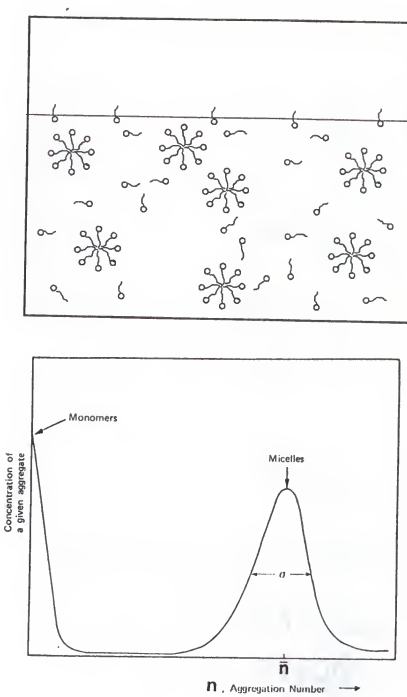

Figure 1-2 The diagram for the aggregate of surfactant molecules (above) and the typical curve for the concentration of a given aggregate vs. their aggregation number (below) in solution.

larger than one. Therefore, micellar lifetime is approximately equal to $n\tau_2$.[13]

1.2 Measurement of Relaxation Time

1.2.1 Introduction

The distribution curve of surfactant molecules in the solution (Figure 1-2) is a function of thermodynamic variables such as temperature, pressure, concentration of surfactant, etc. Therefore, a change in any one of thermodynamic variables will cause a change in the characteristics of distribution curve such as monomer concentration, micellar aggregation number, the number of micelles and half width (σ) of the curve.[8]

Micellar lifetime can be measured by monitoring that how fast the micellar solution reaches a new equilibrium state after a sudden change in any one of the thermodynamic variables.[14] If the micellar lifetime is short, the micellar solution will reach a new equilibrium state very quickly due to a quick formation or breakdown of micelles. The methods used to measure micellar lifetime are classified according to which thermodynamic variable is changed suddenly. The stopped-flow (or concentration-jump) method uses a sudden change in the concentration of surfactant, the temperature-jump method uses a sudden change in temperature, and the pressure-jump method uses a sudden change in pressure of the solution.

1.2.2 Stopped-flow method

A surfactant solution is rapidly mixed either with pure solvent or with a second solution having a different concentration or ionic strength. Useful results can be obtained if one or more of the subsequent reactions is relatively slow with a relaxation time no shorter than about 1 msec,[15] because the mixing time is usually of this order. Changes in electrical conductivity or optical properties of the solution have been used to measure the relaxation time. If the change in optical properties of the sample is monitored for a relaxation process, it may require the addition of an appropriate dye having an absorption spectrum showing characteristic changes when it is transferred from an aqueous to a micellar environment.

1.2.3 Jump methods

A solution, originally at equilibrium, is perturbed by a sudden change in an external variable (i.e., temperature in temperature-jump, pressure in pressure-jump) which derives it to a new equilibrium from the original equilibrium state. The subsequent attainment of the new equilibrium state of micellar solution is monitored by observing the time dependence of some convenient property such as electrical conductivity or optical density at a specific wavelength. The lower limit on the relaxation time which can be accurately measured depends on the time required to impose the initial perturbation. In a typical pressure-jump, the pressure falls during an interval of 50-100 μsec following the rupture of a metal diaphragm.[15] In a

temperature-jump, the typical heating time is 5 to 50 μsec. The fast heating method in the temperature-jump technique uses single-shot square-wave voltage pulses with rise and fall times of about 10 nanoseconds to create electric discharge and a subsequent rise in temperature.[16]

1.3 Factors affecting the micellar relaxation time

1.3.1 Chain length of surfactant

In the alkylsulfate series, the CMC decreases by two orders of magnitude in going from the decyl to the hexadecyl compound, and since A_1 is equal to the CMC, this would account for the increase in $1/\tau_2$ (equation 1.1). The aggregation number (n) also increases as the chain length of surfactants increases,[17] so that the n^2 term in equation (1.1) would contribute another rate increase, about sixfold. But the observed change is a decrease of about four and a half orders of magnitude.[18] This must reflect an overwhelming increase in R. Conceptually, the attraction force between the hydrophobic tails of surfactant molecules increases as the chain length increases. This increased attraction force between surfactant molecules contributes to the increases in τ_1 and τ_2 values of surfactants with the chain length as shown in figure 1-3 for sodium alkyl sulfate surfactants.[19]

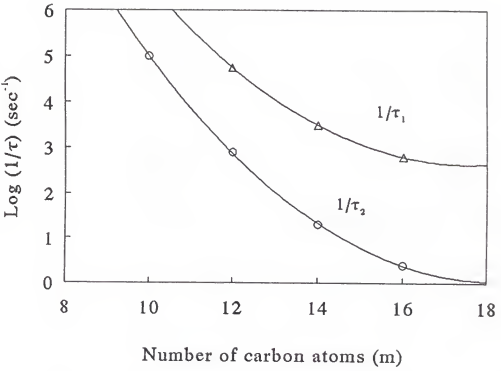

Figure 1-3 Plot of $\log(1/\tau_1)$ and $\log(1/\tau_2)$ vs. the number m of carbon atoms of the hydrophobic tail for several sodium alkyl sulfates at 25 °C at CMC.

1.3.2 Temperature

τ_1 and τ_2 decrease as the temperature increases due to increases in thermal motion of molecules with temperature in the micelles, which is the driving force for micellar dissociation. Figure 1-4 and 1-5 show the effect of temperature on τ_1 and τ_2 values of sodium tetradecyl sulfate at various concentrations.[19]

1.3.3 Salt effect (NaCl)

The τ_2 values of ionic surfactants are extremely sensitive to a change in added salt concentration. Salt addition tends to increase the aggregation number (n) and decrease the monomer concentration (i.e., decrease in CMC),[17] resulting in the change in R according to equation (1.3). The law of mass action requires that for each aggregate A_s is proportional to $(A_1)^s$, and since electrolyte addition depresses the CMC this accounts for a large increase in R. Also the addition of electrolyte decreases the electric repulsion between surfactant molecules in the micelles. Therefore, τ_1 and τ_2 increase with the addition of electrolyte. Figure 1-6 shows the change in τ_2 value of sodium tetradecyl sulfate (CMC=2.1 mM) with salt concentration. The slow relaxation time also increases as the salt concentration increases.[19]

1.3.4 Chain length of solubilized alcohol

The slow relaxation times of SDS are found to decrease for all alkanols except

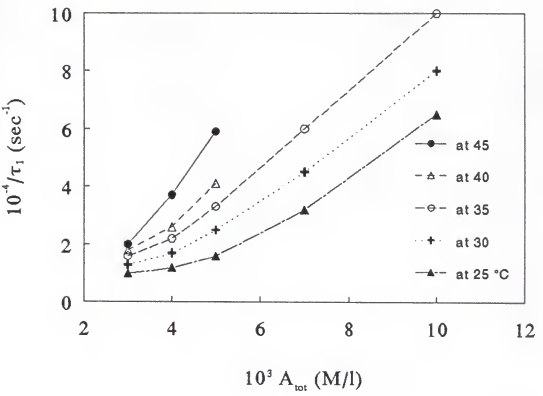

Figure 1-4 Plot of $1/\tau_1$ vs. surfactant concentration for STS at different temperatures.

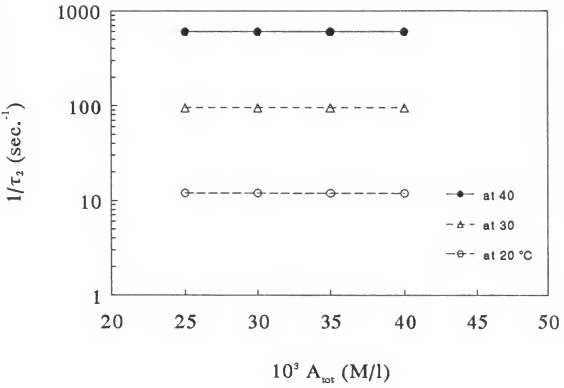

Figure 1-5 Plot of $1/\tau_2$ vs. surfactant concentration for STS at different temperatures.

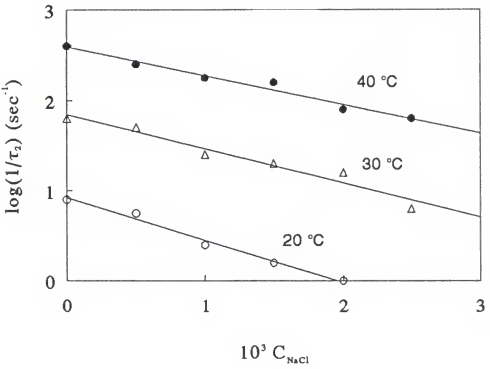

Figure 1-6 Plot of $\log(1/\tau_2)$ vs. the concentration of added NaCl for STS with A_{tot} = 2.3 X 10^{-3} M at different temperatures.

pentanol at which a reverse trend is observed. This indicates that short chain alcohols from C_1 to C_4 labilize micelles, but C_5 alcohol stabilizes micelles (Figure 1-7).[13] These results can be explained as follows. It is likely that short-chain alcohols with three carbons or fewer mainly partition in the palisade layer, where the microenvironment of alcohols is probably not much different from the bulk water. Hence the exchange of alcohols between bulk phase and micellar phase is extremely fast without much hinderance. The measured relaxation rate is mainly due to the micellization kinetics of surfactant molecules. However, as the alcohol chain length increases to four carbons or more, alcohols start penetrating into the hydrocarbon core of micelles. The exchange of alcohol between the micelles and the bulk solution will then be hindered and slowed down. Therefore, the relaxation rate reflects partly the rate of solubilization of alcohols into micelles.[13,20]

1.3.5 Chain length of oil solubilized

The addition of oil usually produces an increase in τ_2 except in the case of toluene, which first induces a decrease in τ_2 as in the case of addition of C_5 alcohol into SDS solution, and then, for higher toluene concentration, induces an increase in τ_2. It is well known that toluene, just like other aromatic molecules, when added to a micellar solution, goes into the palisade layer of the micelle at low concentrations. At higher concentrations, toluene is also dissolved in the core of micelle.[21] Thus the behavior of the toluene is like that of C_5 alcohol (Figure 1-8).

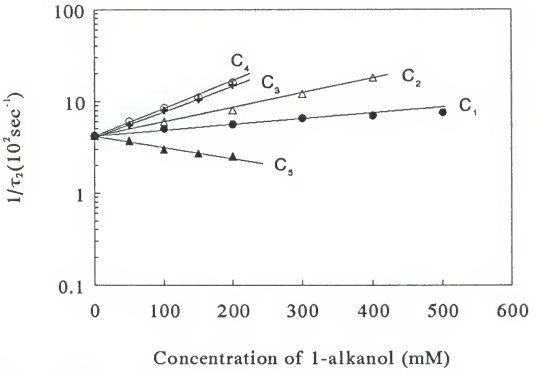

Figure 1-7 Variation of the slow relaxation time $1/\tau_2$ of 10 mM SDS as a function of alkanol concentration.

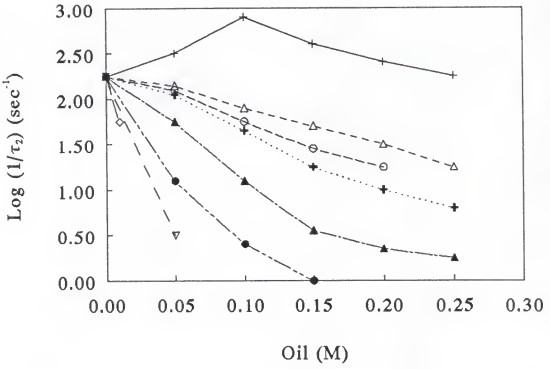

Figure 1-8 Plots of $\log(1/\tau_2)$ vs. the concentration of various oils added to 0.3 M HPyrC + 0.2 M 1-pentanol mixed micellar solutions at 25 °C. The curves for toluene, cyclohexane, butylbenzene, hexane, heptane, nonane, dodecane and tetradecane are shown from the top to the bottom.

1.3.6 Effect of polymeric additive

It has been reported that the $1/\tau_2$ value of micelles at 100 mM SDS concentration showed a three-orders-of-magnitude increase as nonionic polymer polyvinylpyrrolidone (PVP) concentration increased from 1 to 8 weight % (Figure 1-9). The presence of polymer does not alter the micellization characteristics of SDS significantly, hence the steep increase in $1/\tau_2$ in figure 1-9 can be interpreted in terms of the effect of polymer on micellization kinetics of SDS. In analogy to a heterogeneous nucleation process, PVP is likely to act as a nucleating agent for surfactant and stabilize the micelle nuclei in the solution.

1.4 Slow Relaxation time of Sodium Dodecyl Sulfate

1.4.1 Measurement of τ_2 of SDS micelles

Sodium dodecyl (C_{12}) sulfate, supplied by Sigma Chemical Company (purity 99 %), and double-distilled water were used to make micellar solutions. Hexanol, supplied by Eastman Kodak Company (purity 99 %) was added to SDS micellar solutions to study the micellar stability of mixed micelles. The second relaxation time (τ_2) of micelles was measured by the pressure-jump apparatus with conductivity detection from Dia-Log Corporation (Dusseldorf, Germany) with a pressure-jump of 140 bar at 25 °C (Figure 1-10).

A KCl solution having the same electrical conductivity as that of the surfactant

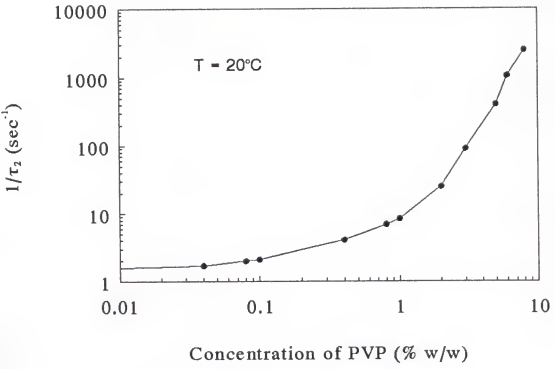

Figure 1-9 Variation of the slow relaxation time $1/\tau_2$ of 100 mM SDS solution as a function of PVP concentration.

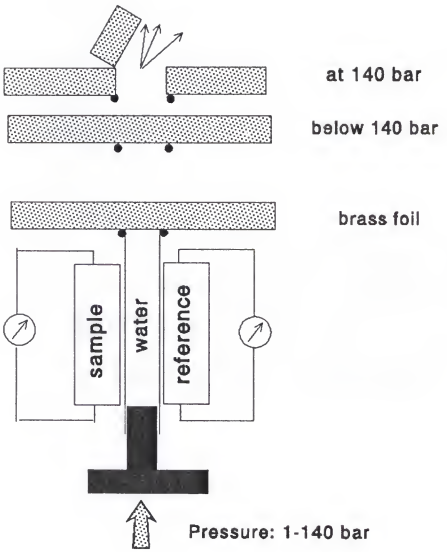

Figure 1-10 Sectional views of the pressure-jump apparatus with conductivity detection.

solution was used as a reference cell in the pressure-jump experiment.[13] The micellar solution, originally at equilibrium, is perturbed by a sudden pressure drop from 140 bar to 1 bar. Then, the micelles will reaggregate to reach a new equilibrium state. This subsequent return to equilibrium is monitored by observing the time-dependence of electrical conductivity of the solution. The CMC of surfactant in aqueous solution increases as the pressure increases.[22] Therefore, the electrical conductivity of SDS solution decreases as the pressure decreases from 140 bar to 1 atm because the monomer concentration of SDS at 140 bar is higher than that at 1 atm (Figure 1-11). If the micelles are very stable, it will take a long time for micelles to reaggregate and reach a new equilibrium state after the sudden change in pressure. Therefore, the electrical conductivity of solution will decay very slowly. The relaxation time of micelles can be calculated from the decay curve of electrical conductivity as a function of time. Figure 1-12 shows electrical conductivity change of a 200 mM SDS solution with the abrupt change of pressure from 140 bar to 1 bar.

The relaxation amplitudes in pressure-jump machine first decrease with increasing surfactant concentration, becoming rather small within a limited concentration range, but then increase again with further increasing concentration to approach an apparently constant value which is proportional to $(\partial \ln m/\partial P)_T$, where m denotes the mean aggregation number of the proper micelles. As long as $(\partial \ln m/\partial P)_T$ is different from zero, the relaxation measurements can be extended to high

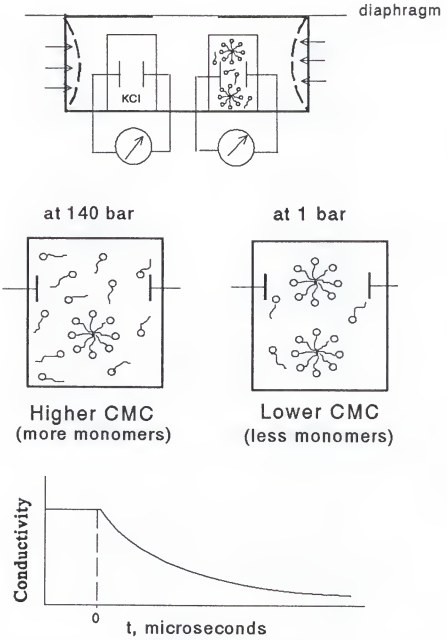

Figure 1-11 The expanded diagram for the solution cells in the pressure-jump machine and the microscopic behavior of micellar solutions with the abrupt pressure change, followed by the electrical conductivity change of solution.

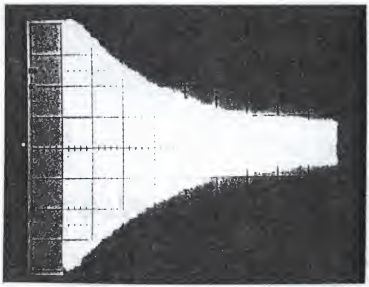

Figure 1-12 The decay curve of electrical conductivity at 200 mM SDS concentration in pressure-jump machine (1 division is 1.0 second).

concentration.[23]

The slow relaxation time τ_2 of SDS micelles showed a maximum at 200 mM of SDS concentration (Figure 1-13), indicating that most stable SDS micelles are formed at this concentration. Similar study has been reported by Lessner and Frahm[24] for the relaxation time of cesium dodecyl sulfate (CsDS) using pressure-jump technique. The most stable micelles of CsDS were formed at 100 mM surfactant concentration. The τ_2 values of CsDS micelles were in the range of 0.001 - 10 seconds, similar to those of SDS micelles (0.005 - 10 seconds).

1.4.2 Fragmentation Model

Kahlweit[25] explained the maximum relaxation time of SDS micelles at 200 mM concentration on the basis of the difference in micellar formation and dissociation mechanism. Below 200 mM SDS concentration, the main mechanism of micellar kinetics is

$$A_{i-1} + A_1 = A_i$$

Micelles are dissociated completely by the removal of surfactant monomers one by one from the micelle. On the contrary, the main mechanism of micellar kinetics above 200 mM SDS concentration is

$$A_k + A_m = A_i, \quad k + m = i$$

where (k) and (m) are classes of submicellar aggregates. Micelles are dissociated by the removal of submicellar aggregate at one time from the micelle.

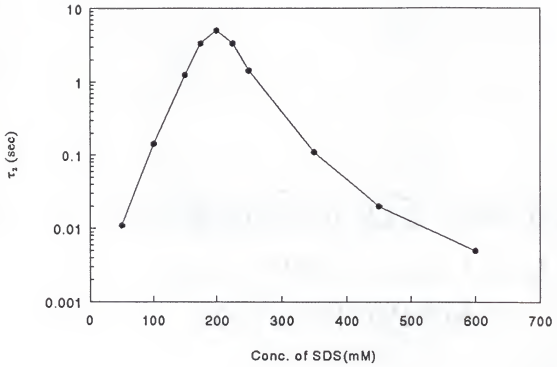

Figure 1-13 The slow relaxation time (τ_2) vs. SDS concentration.

However, the formation of most stable micelles at 200 mM SDS concentration in our study can be explained by the following proposed Intermicellar Coulombic Repulsion Model (ICRM).

1.4.3 Intermicellar Coulombic Repulsion Model (ICRM)

The intermicellar distance in SDS solution decreases as the surfactant concentration increases due to the increase in the number of micelles. The intermicellar distance was calculated as follows:

Let us divide the solution into cells (or cubes) of the same volume, and the number of cubes being the same as the number of micelles. Each cube contains a micelle as shown in figure 1-14. The number of micelles (N_m) in the solution is given by;

$$N_m = \frac{(C_{tot} - CMC) \cdot A_o}{n} \qquad (1.4)$$

where C_{tot} is the total concentration of surfactant (moles/l), A_o is the Avogadro number and n is the aggregation number of the micelle. If the volume of surfactant solution (V) is 1 liter (i.e., 1000 x 10^{24} Å^3) then the volume of the cell occupied by each micelle is V/N_m. Therefore, the average intermicellar distance (ℓ) or the length of the cube is given by $(V/N_m)^{1/3}$.

The intermicellar distance using this procedure at various SDS concentrations is shown in figure 1-14 when the aggregation number of micelle is 64.[26] The intermicellar distance at 50 mM SDS concentration is 130 Å, which is equivalent 3.6 times the micellar diameter,[27] but at 200 mM concentration the distance is 78.6 Å, which is equivalent to approximately twice the micellar diameter (40 Å). It is possible that the binding of sodium ions to micelles increases to decrease the coulombic repulsion between micelles as they come closer and hence the stability of micelles increases. It appears that micelles pack rather closely in the SDS solution at 200 mM concentration. Above 200 mM SDS concentration, the structural transition from spherical to cylindrical occurs to accommodate more surfactant molecules into the solution and minimize the free energy of the system. Moreover, Ekwall[28] has shown that the transition from spherical to cylindrical micelles occurs in a wide range of concentrations. As this structural transition proceeds, the concentration of spherical micelles decreases, and hence the intermicellar distance between spherical micelles increases. It should be noted that cylindrical micelles are likely to be more stable than spherical micelles. Hence, in solutions containing both the spherical and cylindrical micelles, the relaxation time is predominantly determined by the spherical micelles because spherical micelles are more labile structures compared to cylindrical micelles. Since the intermicellar distance between spherical micelles increases in such systems (above 200 mM SDS, figure 1-14-D), the relaxation time decreases due to less coulombic repulsion between spherical micelles.

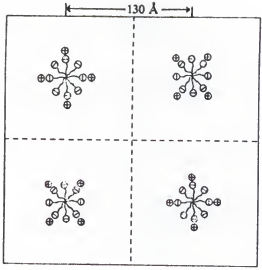

(A) at 50 mM

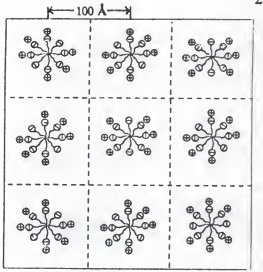

(B) at 100 mM

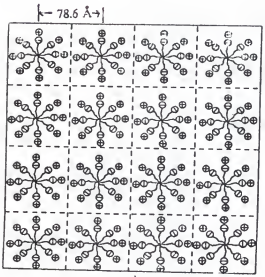

(C) at 200 mM

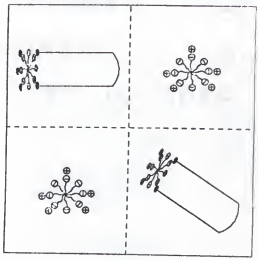

(D) above 200 mM

Figure 1-14 Packing model for SDS micelles at various surfactant concentrations.

At well above CMC, micellar life-time is equal to $n\tau_2$.[29] The aggregation number n of SDS micelles changes from 63 to 91 as the concentration increases from 0.07 to 0.73 M.[30] This change of aggregation number is negligible when it is compared with the change of τ_2 value (0.001 to 10 seconds) in the experimental concentration range. Therefore, the slow relaxation time (τ_2) represents directly the lifetime (i.e., stability) of micelles.[13]

CHAPTER 2
THE RELATIONSHIP BETWEEN MICELLAR LIFETIME AND FOAMABILITY OF SDS AND SDS/1-HEXANOL MIXTURES

2.1 Introduction

Foam is a term for dispersions of gas in liquid in which the volume fraction of the dispersed phase is so high that the "colloid" in the system might well be regarded as the network of interconnected films.[4] Foam is produced when gas is injected into a solution containing surfactants due to the adsorption of surfactants on the newly created surface.[17] Foam cannot be formed from pure liquids. This fact can be confirmed by a thermodynamic argument. A foam has dramatic surface area to make its surface free energy a significant contribution to the total energy of the system. The Helmholtz function for foam should, therefore, include surface area as an extensive variable:[31]

$$dF = -pdV - sdT + \gamma dA + \Sigma \mu_i dn_i \qquad (2.1)$$

where γ is the surface tension of the liquid, A its total surface area, and μ and n refer to the chemical potentials and concentrations, respectively, of its various

components. Integration of equation (2.1) at constant temperature and concentration gives:

$$\Delta F = \gamma \Delta A - \int p dV \qquad (2.2)$$

Equation (2.2) applied to a foam shows that a decrease of the free energy results both from a loss of area and from an expansion of the gas, both of which come about by coalescence of bubbles: hence, a foam composed of gas in a pure liquid is thermodynamically unstable. The foams that can remain stable for an appreciable time are not created from pure liquids. The third component, which is usually a solute in the liquid, although it may also be a finely divided solid,[32] a liquid-crystal[33] phase, or an insoluble monolayer,[34] is necessary to make foam. This foam stabilizer must be surface active, i.e., it must spontaneously adsorb at the liquid surface. If it is a finely divided solid particle, it must remain at the surface by virtue of a finite angle of contact with the liquid.

The foamability and foam stability of the surfactant solutions are primarily dependent on the chemical composition and properties of the adsorbed surfactant molecules and are influenced by numerous factors such as the rate of adsorption from solution to the liquid-gas interface, the rheology of the adsorbed layer, gaseous diffusion out of and into bubbles, size distribution of bubbles, surface tension of liquid, bulk viscosity of liquid, microstructure of foaming solution, the presence of

electrolyte as well as external temperature and pressure.[35-39]

The liquid film stability in foam can be studied using the disjoining pressure (π_D) introduced by Deriaguin and co-workers in a quantitative manner. The disjoining pressure is defined as[40]

$$\pi_D = -(\frac{\partial(G/A)}{\partial h})_{T,S} \tag{2.3}$$

the partial derivative of the free energy (G) per unit area (A) of film with respect to thickness (h) at constant temperature (T) and entropy (S) with a negative sign so that a positive pressure favors thinning process. This disjoining pressure (π_D) can be split into several components such as electrical double layer (π_e), van der Waals (π_{vdW}), structural (π_s) and other parts (π_o):

$$\pi_D = \pi_e + \pi_{vdW} + \pi_s + \pi_o \tag{2.4}$$

π_e is positive and electrical repulsion due to overlapping of diffuse double layers in case of charged surface that opposes drainage of liquid. π_{vdW} is negative, van der Waals force between surfactant layers in the film that promotes thinning. π_s is due to the alternation of solvent structure in the boundary layer and π_o is all other contributions to π_D.

When this disjoining pressure (π_D) is equal to zero, the thinning of liquid film stops,

and the film thickness will reach the equilibrium value.[41]

The foam stability is increased as the bulk viscosity of foaming solution and surface viscosity of the adsorbed surfactant layer at the air/water interface are increased.[42] In contrast, the foam stability tends to decrease as the size distribution of bubbles, surface tension of solution, area/molecule of surfactant molecule and diffusion coefficient of gas through the liquid film increase.[43-47] If the size distribution of bubbles is broad, the pressure difference between small and large bubble causes a concentration gradient in the liquid layer separating the bubbles. As a result of this concentration gradient, transport of gas will take place from smaller to a larger bubble. The larger bubble will grow at the expense of the smaller one, and the smaller bubble will eventually disappear. Consequently, a coarsening of the foam will take place. Also the foam stability decreases in the presence of electrolytes because the electrical repulsion between the ionic surfactant molecules at the interface decreases.[48,49]

Wasan et al.[50] observed stratification during the thinning of liquid films formed from micellar solutions of anionic surfactants. They explained that the stepwise thinning occurs due to the layer-by-layer removal of an ordered structure of micellar layers from the film. The thickness of each thinning step is of the order of the diameter of a micelle together with the Debye atmosphere around it. The gradient of the chemical potential of micelles at the film periphery causes the stepwise thinning of the film.[51] The foamability (i.e., the volume of foam generated) is

reported to increase with the temperature and decrease with the surface tension of the surfactant solutions.[52,53]

The foaming ability of organic solvents carried out by Ross, et al. showed simple rules for the tendency to form transient forms of organic solutions or emulsions of two immiscible solvents. For organic solutions, foaming increases when the composition approaches the limit of solubility. The foaming of the two-phase system takes place only when the phase with higher surface energy is the continuous one. For that case, the foaming ability increases with reduced amounts of the dispersed phase present, so that the foaming ability is a continuous function of composition across the solubility limit. The part of the compositions, which give the low surface tension phase as the continuous one in the emulsion, no foaming was found.[54]

In this study, it has been shown that the foamability of micellar solutions is influenced by the average lifetime of micelles. This happens because the micelles must be broken into monomers for adsorption onto the newly created surfaces of the bubbles (Figure 2-1). Without this process, foam can not be generated. If the micelles in solution are very stable, they cannot rapidly provide surfactant monomers to the newly created surface. Hence, foaming ability would be poor. But if the micelles are relatively unstable, their disintegration provides the surfactant monomers which can rapidly adsorb to the newly created surface. This should enhance the

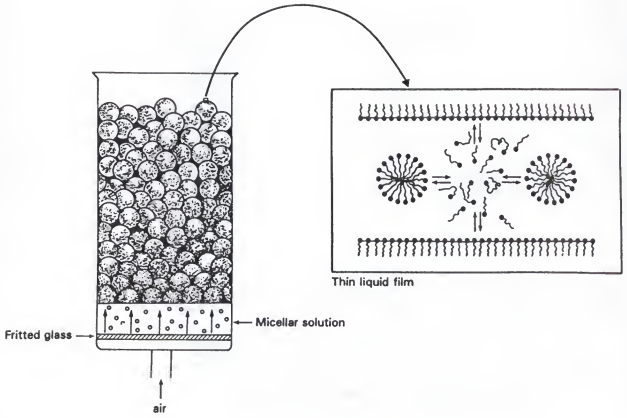

Figure 2-1 A schematic representation of adsorption of surfactant monomers to the expanding interface due to the disintegration of micelles during the foam generation.

foamability of micellar solutions, but the effect of micellar lifetime on foamability of micellar solutions has never been considered or established.

In this study, the effect of micellar lifetime on foamability of sodium dodecyl sulfate and mixtures of SDS and 1-hexanol was studied by the pressure-jump technique and air-blowing foam column to establish the mechanism of foam generation process.

2.2 Experimental Procedure

The 1-hexanol (Eastman Kodak Company, >98 % purity) was added to 50 and 100 mM SDS solutions until phase separation occurred, respectively. The phase separation occurred at 250 mM and 300 mM of 1-hexanol concentration, respectively, at 25 °C. The second relaxation(τ_2) of SDS and SDS/1-hexanol mixed micelles was measured by pressure-jump technique as described in chapter 1. The foamability of SDS and SDS/1-hexanol solutions (5 ml) was measured at various SDS concentrations in the air-generated foam column with diameter 5 cm. The foam heights were read after 30 seconds of air flowing at P=2 psig through the column as shown in figure 2-1. All measurements were carried out at 25°C.

2.3 Results and Discussion

As shown in figure 1-12, the slow relaxation time (τ_2) of SDS micelles increased as the surfactant concentration increased up to 200 mM concentration and then decreased with concentration. This suggests that the lifetime of SDS micelles in aqueous solution is maximum at 200 mM SDS concentration. The foamability of SDS solutions in the air-blowing foam column was at a minimum at 200 mM concentration probably because surfactant monomers can not be provided by relatively stable micelles (Figure 2-2). Thus, it seems that the more stable the micelles, the less is the foamability of the micellar solutions.

It is important to establish that the diffusion time of surfactant monomers from bulk to the surface in thin films during the foam generation process is much shorter than the lifetime of micelles. Thus, the lifetime of micelles can be considered as the rate limiting step in a foam generation process. Overbeek[55] has derived an approximate equation for the diffusion-time of molecules based on the Stokes-Einstein equation:

$$t_{Dif.} = \frac{(Diffusion\ \ Path\ \ Length)^2}{2D} \qquad (2.5)$$

where D is the diffusion coefficient of molecules. When the film thickness is 1 μm, the average diffusion path length of surfactant inside the liquid film is 0.25 μm as

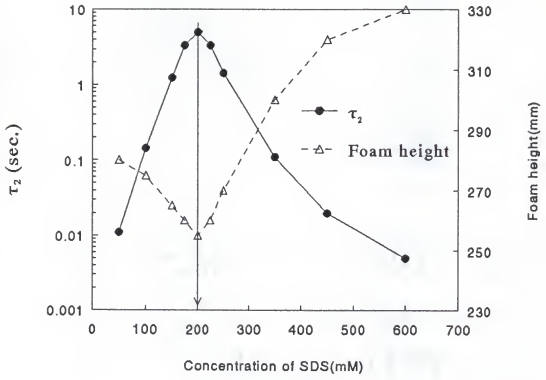

Figure 2-2 The effect of concentration of SDS on the micellar relaxation time and foaming ability.

explained below. The molecules diffuse towards both sides of the films. Hence, only half of the film (0.5 μm) is able to provide monomers to one side of the film. In half of the film the average path length travelled by molecules is 0.25 μm. In this case, the average diffusion time of surfactant monomers calculated by equation (2.5) is 10^{-4} second. This value is negligible when it is compared with the micellar lifetime ($n\tau_2$, 0.6-65 seconds) of SDS micelles. Therefore, the rate of diffusion of surfactant monomers inside the thin liquid film does not influence the foamability of surfactant solutions in the air-generated foam column. Thus, it can be concluded that the micellar stability plays a major role in foamability of micellar solutions.

It was reported that the short chain alcohols (C_1 to C_4 chain length) labilize the SDS micelles (i.e., decrease τ_2) in aqueous solutions as the concentration of alcohols increases.[13] In contrast, Inoue et al.[56] showed that SDS micelles are stabilized by the addition of a small amount of dodecyl alcohol.

The effect of addition of 1-hexanol to 50 mM and 100 mM SDS solution on the micellar lifetime (i.e., relaxation time τ_2) and the foaming ability is shown in Figures 2-3 and 2-4 respectively. The slow relaxation times of SDS/1-hexanol mixed micelles were maximum at 70 mM concentration of 1-hexanol in 50 mM SDS solution and 50 mM 1-hexanol in 100 mM SDS solution, respectively. The foamability also showed a minimum at these concentrations.

From these results, it can be concluded that the surfactant solutions which

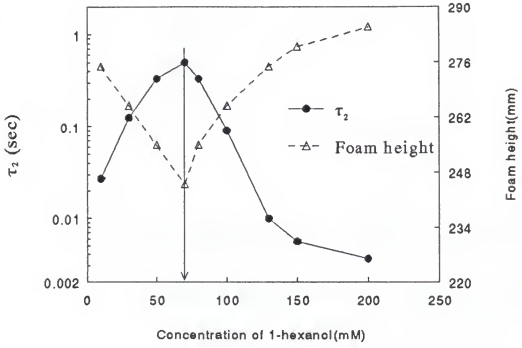

Figure 2-3 The effect of concentration of 1-hexanol on the micellar relaxation time and foaming ability of 50 mM SDS solution.

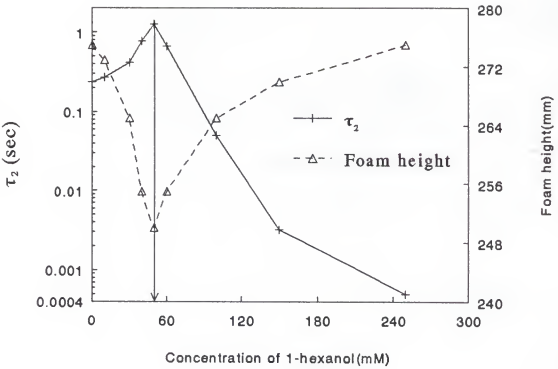

Figure 2-4 The effect of concentration of 1-hexanol on the micellar relaxation time and foaming ability of 100 mM SDS solution.

exhibit greater relaxation time (i.e., longer lifetime or greater stability) yield poorer foamability. It can be postulated that the rate of adsorption of surfactant monomers onto the newly created surface during the foam generation process is primarily dependent upon the disintegration of micelles. These results are relevant to the processes encountered in detergency, enhanced oil recovery by foam flooding, wetting of textile fibers, ore flotation, etc.

It should be emphasized that this study deals only with the foaming ability of surfactant solutions and not with foam stability. It is well recognized that the addition of long chain alcohols to the SDS solution increases the stability of foams.[57] This effect can be attributed to the shielding of the negative charges of SDS with hydroxy groups (-OH) of alcohol molecules and a possible stabilizing effect of ion-dipole interactions between sulfate and hydroxy groups.

In summary, the results described in this study suggest that the stability (or relaxation time τ_2) of micelles correlates with the foamability of the micellar solutions. The minimum foamability occurs when the micellar solution exhibits a maximum in the relaxation time (i.e., micellar stability).

CHAPTER 3
THE EFFECT OF MICELLAR LIFETIME ON THE BUBBLE DYNAMICS IN SDS SOLUTIONS

3.1 Introduction

For surfactant applications such as detergency, wetting, coating of solids and bubble generation, the process time is often less than the time required for the surface (or interfacial) tension to reach equilibrium.[58] In these cases, the dynamic surface tension of surfactant solutions plays a more important role in the processes rather than the equilibrium surface tension.[17] The dynamic surface tension can be measured by the drop weight,[59,60] oscillating jet,[61] capillary wave,[62] growing drop technique[63] and maximum bubble pressure methods[64,65]. Rosen et al.[66] showed that the dynamic surface tension of surfactant solutions decreases more rapidly as the concentration of surfactant or the temperature increases. Ward et al.[67] reported that the dynamic surface tension of SDS solution increases as the frequency of bubble formation increases due to the decreased adsorption of monomers from the bulk to the surface below the CMC.

During the bubble growth, surfactant monomers adsorb from the bulk to the

expanding surface (Figure 3-1). The bubble detaches itself from the tip when the buoyancy force exceeds the surface tension force at the tip/bubble interface. The following expression relates the dynamic surface tension (γ) with the radius of capillary (r), radius of bubble (R) and the density difference between the liquid and gas (ρ).[35]

$$R^3 \alpha \frac{3r\gamma}{2g\rho} \tag{3.1}$$

The bubble size decreases as the dynamic surface tension decreases. Also the frequency of bubbles increases as the dynamic surface tension decreases if the flow rate of air is kept constant. The various bubble shapes such as spherical, ellipsoidal, spherical cap, or wobbling have been observed.[68] They showed that bubble shape depends on the dynamic surface tension of the bubble surface as well as on the viscosity and density of the solution.

The growth of a bubble in the surfactant solution below and above CMC can be viewed as follows. Below the CMC, the surfactant monomers diffuse to the bubble surface as the bubble grows. However, above CMC, the diffusion of monomers is augmented by the spontaneous breakdown of micelles as the monomers are depleted from the vicinity of the micelles. The bubble dynamics is controlled mainly by the diffusion process below the CMC.[69] In case of diffusion-controlled process, the adsorption kinetics at the surface of a growing bubble can be described

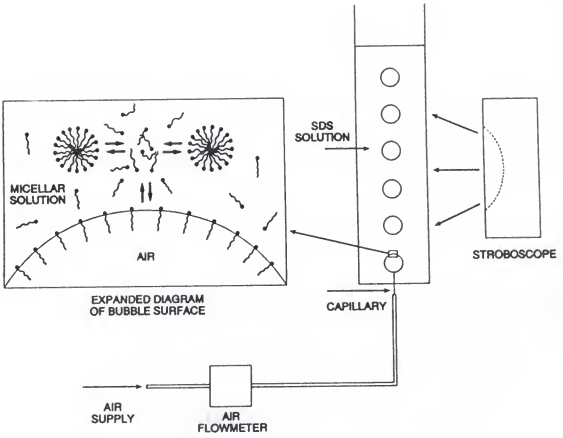

Figure 3-1 An experimental apparatus and expanded diagram for the adsorption of surfactant monomers from micellar solution to the expanding interface by disintegration of micelles during bubble formation.

by a modified Ward and Tordai equation:[70]

$$\Gamma(t)=\Gamma_o+2C_o(3\frac{Dt}{7\pi})^{\frac{1}{2}}-(\frac{D}{\pi})^{\frac{1}{2}}t^{-\frac{2}{3}}\int_0^{\frac{3}{7}t^{\frac{7}{3}}}\frac{C_s(\frac{7}{3}\lambda^{\frac{3}{7}})}{(\frac{3}{7}t^{\frac{7}{3}}-\lambda)^{\frac{1}{2}}}d\lambda \qquad (3.2)$$

where $\Gamma(t)$ is the surfactant concentration at the surface at time t, Γ_o is the initial surfactant concentration, C_o is the bulk concentration of surfactant, D is the diffusion coefficient, C_s is the subsurface concentration of surfactant, and λ is a dummy variable.

As the concentration of surfactant increases, the micellar stability also increases as indicated by the relaxation time τ_2 up to a specific concentration (e.g., 200 mM for SDS solution).[13] Beyond this concentration, τ_2 decreases. The previous chapter reported that the life-time of micelles correlates with the foaming ability of surfactant solutions.[71]

The mathematical model has been proposed by Fainerman and Makievski for the effect of micellar lifetime on the dynamic surface tension of the solution, which is a major governing factor of bubble dynamics.[72] The dynamic surface tension of

micellar solutions at high surfactant concentration does not depend on the total surfactant concentration. Rather, it depends on the slow dissociation process of micelles.[73]

The present study reports the effect of the diffusion of monomers on the bubble dynamics in the presence or the absence of micelles in SDS solutions. Furthermore, this study also reports the effect of micellar stability on the bubble dynamics in SDS solutions.

3.2 Experimental Procedure

The frequency of bubble formation was measured in a column with a diameter of 4.7 cm and a liquid height of 11.7 cm at 25°C as shown in figure 3-1. The air flow-rate was controlled by a flowmeter (Matheson Inc., tube size R-2-15-AAA) at 230 ml/min. The diameter of capillary was 1 mm. The stroboscope supplied by Cenco Company was used to measure the frequency of bubble formation. When the frequency of the blinking light in the stroboscope is the same as the frequency of bubble formation in column, bubbles appear to be stationary. But bubbles may appear to be stationary at several frequencies of stroboscopic light. The frequency of stroboscopic light was taken as the bubble frequency when the number of bubbles in the column with and without stroboscopic light is the same.[74]

3.3 Results and Discussion

Figure 3-2-A shows the effect of SDS concentration on the bubble radius and frequency. The CMC of SDS is reported to be 8 mM. Thus, the bubble size was fairly large (~ 0.64 cm of radius) below CMC. However, as the SDS concentration approaches the CMC, the bubble size decreases and reaches a minimum radius at 50 mM. Then the bubble radius increases up to 200 mM and subsequently decreases. Figure 3-2-B shows the relaxation time τ_2 of the micelles in this concentration range. It is interesting that the relaxation time τ_2 also exhibits a maximum at 200 mM of SDS concentration. There is no significant change in τ_2 in the range 8 to 50 mM of SDS.[52] The bubble dynamics and relaxation time τ_2 as a function of SDS concentration have been interpreted as follows.

From 10^{-3} mM to 1 mM SDS concentration, the bubble size is large because of high surface tension at the bubble surface. Between 1 to 50 mM of SDS concentration, the bubble size decreases because of the additional supply of SDS monomers due to spontaneous breakdown of micelles as the monomers diffuse to the bubble surface (Figure 3-3-A). As the concentration of micelles increases, the flux of monomers to the bubble surface is also expected to increase (Figure 3-3-B). It should be noted that the micellar stability or τ_2 in this range (8-50 mM) remains relatively constant (Figure 3-2-B). However, from 50 to 200 mM of SDS concentration, τ_2 increases strikingly due to the increase of micellar stability.

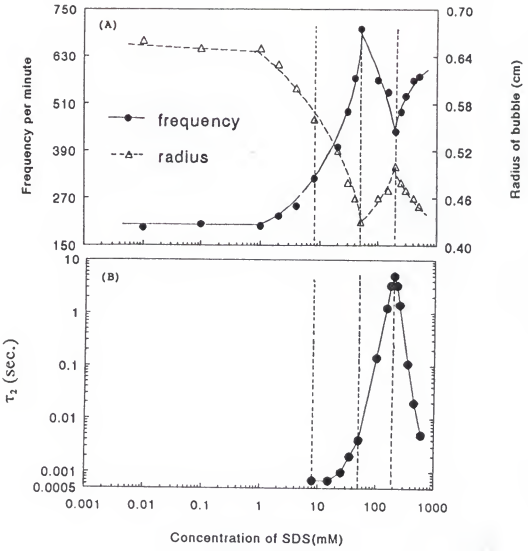

Figure 3-2 The effect of micellar relaxation time on the frequency of bubble formation and bubble size in SDS solution.

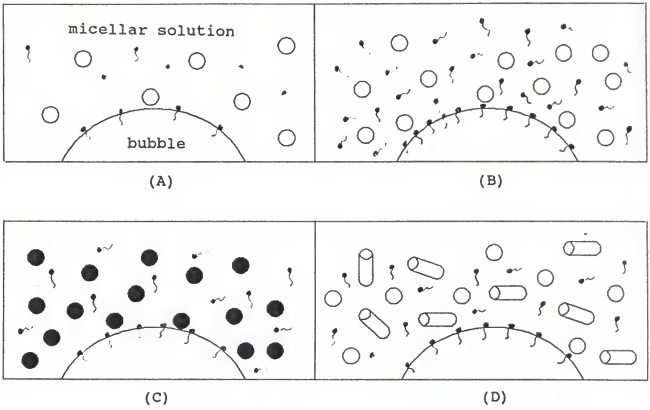

Figure 3-3 The schematic diagram of monomer and micellar concentration near the bubble surface. (A) is at 8 mM, (B) is at 50 mM, (C) is at 200 mM and (D) is at 400 mM.

Concomitantly, the bubble size also increases because relatively stable micelles do not augment the flux of monomers to the bubble surface (Figure 3-3-C).

Since the flow-rate of air was maintained constant, larger bubble size corresponds to a less frequency of bubble generation. Thus, our frequency of bubble is the reverse of the bubble size as a function of SDS concentration (Figure 3-2-A).

It is desirable to estimate the diffusion time of surfactant monomers from the bulk to the bubble surface during the bubble generation process as compared to the life-time of micelles.

3.4 Calculation of Diffusion Length (L_D) and Characteristic Diffusion Time (T_D) for Saturation of the Bubble Surface by SDS Monomers

As shown in Figure 3-4, surfactant monomers near the bubble surface diffuse from the bulk to the surface. The number of monomers (N_1) needed to saturate the bubble surface of radius R_1 can be calculated by the following equation:

$$N_1 = \frac{4\pi R_1^2}{A} \tag{3.3}$$

where A is the area/molecule of surfactant at the air/water interface. The number of molecules per ml of solution (N_2) at CMC (in unit of moles/liter) is CMC x (Avogadro number)/1000. The volume around the bubble which contains N_1

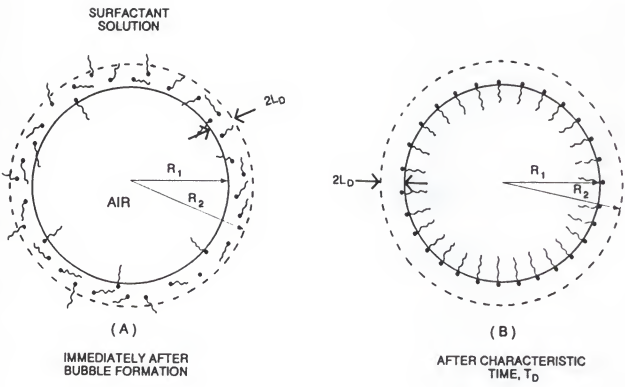

Figure 3-4 The characteristic diffusion length (L_D) around the bubble to saturate a bubble of 4.5 mm radius at CMC.

monomers is given by N_1/N_2 ml. Therefore, a shell of radius R_2 (containing N_1 monomers) can be calculated from the following equation.

$$\frac{N_1}{N_2} = \frac{4}{3}\pi(R_2^3 - R_1^3) \tag{3.4}$$

The only unknown quantity R_2 can be calculated by using the values of N_1, N_2 and R_1. For the bubble of radius 0.45 cm (R_1) in SDS solution, 4.8×10^{14} monomers (N_1) are needed to saturate the surface because the surface area of the bubble is 2.54 cm^2 and the area/molecule at the air/water interface is 53 $Å^2$.[75] Using equation (3.3), the number of monomers per ml (N_2) at the CMC (8 mM) is 48.18×10^{17}. The R_2 value calculated by equation (3.4) is $0.45 + 4.0 \times 10^{-5}$ cm. The characteristic diffusion length (L_D) is (R_2 - R_1)/2. Therefore, the average diffusion path length (L_D) is 2.0×10^{-5} cm. The diffusion time (T_D) calculated using the expression[55] $T_D = (L_D)^2/2D$, is 3.3×10^{-5} second. This is the diffusion time when the solution is assumed to be stationary. In fact, the diffusion time in real situations is much shorter than this value due to the convective motion of solution induced by bubble motion. The diffusion time even in the stationary solution (3.3×10^{-5} sec.) is negligible compared to the lifetime of SDS micelles (0.6-65 seconds) in the experimental concentration range. However, the micellar kinetics can augment significantly the diffusion of monomers in determining the dynamic surface tension and the bubble

dynamics in SDS solutions.

In summary, the frequency of bubble formation in SDS solutions does not change below 1 mM, and increases from 1 to 50 mM because of the increase in the number of micelles of the same life-time, then decreases and showed minimum at 200 mM at which most stable micelles are formed. The frequency increased with concentration after 200 mM because of the structural transition from spherical to cylindrical micelles.

CHAPTER 4
THE EFFECT OF MICELLAR LIFETIME ON THE WETTING TIME OF TEXTILE IN SDS SOLUTIONS

4.1 Introduction

Textile wetting involves the displacement of air in the fiber matrix by surfactant solutions. The kinetics of surfactant adsorption is more important than the equilibrium properties of surfactant solutions for the textile wetting process because the equilibrium conditions are rarely attained during the time allowed for wetting in textile processing.[17] Fowkes observed that the log of the wetting time decreases linearly with the log of the bulk phase concentration of the surfactant below the critical micelle concentration.[76] Electrolytes that decrease the surface tension of surfactant solutions, such as Na_2SO_4, NaCl, KCl, increase the wetting power of ionic surfactant solutions.[77,78] As the temperature of the solution is increased, the chain length for optimum wetting by ionic surfactants generally increases, probably because of the increased solubility of the surfactant at higher temperatures and its decreased tendency to adsorb to the surface.[79] Fowkes also found that the rate of wetting was determined not by the bulk phase concentration of the surfactant, but by the rate of diffusion of the surfactant to the wetting front when adsorption of the surfactant onto

the surface is strong.[76] The surfactants of short alkyl chain length and branched hydrophobic groups are more efficient than the surfactants of long and straight alkyl chains as wetting agents due to their higher diffusion coefficients.[80,81] This is presumably due to the less efficient molecular packing in the micelles of branched chain surfactants which results in relatively unstable micelle formation in the solution. The surfactants which cannot be effectively packed in the micelles have strong wetting power due to the higher rate of mass transfer of surfactant monomers to the interface.[17]

The addition of polyoxyethylenated nonionic surfactant increases the wetting efficiency of anionic surfactant solutions, but decreases that of cationic surfactant solutions. This is due to the increase in the mobility of anionic surfactant monomers in solution and the decrease in the mobility of cationic surfactant monomers by the addition of nonionic surfactants,[82] resulting in rapid diffusion of anionic and slow diffusion of cationic surfactants.

When a piece of a fabric is placed on the surface of a surfactant solution, the solution penetrates into the inter-fiber spaces of the fabric (Figure 4-1). These inter fiber spaces can be considered as the cylindrical capillaries of radius r and length l. For the case of thin fabric, where the gravity effect of the liquid inside the capillary can be neglected, the rate of penetration of a liquid into a capillary (v) is given by

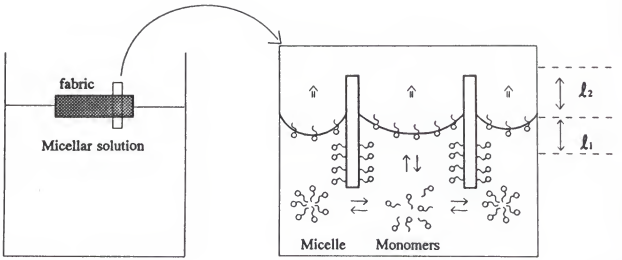

Figure 4-1 Schematic diagram for the adsorption of surfactant monomers from micellar solution to the textile surface by the disintegration of micelles during the wetting process.

the following equation ,[83,84]

$$v = \frac{r\gamma_{L_1L_2}\cos\theta_{sL_1L_2}}{4(\eta_1 l_1 + \eta_2 l_2)} \tag{4.1}$$

where L_1 is a wetting liquid, L_2 is a displaced fluid (air), l_1, l_2 are the length of the capillary filled with the corresponding viscosities of η_1 , η_2 of wetting and displaced fluid (air) and s is the textile.

For textile wetting, the quantity

$$\frac{\gamma_{L_1L_2}\cos\theta}{\eta_1} \tag{4.2}$$

has the dimension of velocity and thus gives a measure of the penetrating power of surfactant solution into the inter-fiber spaces of the fabric.[85] At high surfactant concentrations, the supply of surfactant monomers depends on the breakdown of micelles to provide additional monomers upon depletion of monomers by the adsorption process on the textile fibers. Thus, micellar stability is expected to influence the wetting time of the fabrics.

It is proposed in this study that the wetting time of the fabrics should be influenced by the average lifetime of micelles because the micelles must disintegrate into the monomers for adsorption onto the fiber surfaces. If the micelles in the

solution are relatively stable, they cannot rapidly breakdown and provide additional surfactant monomers to the fiber surfaces. Therefore, the fabric cannot be quickly wetted by the solution. On the other hand, if the micelles are relatively unstable, their rapid disintegration provides additional surfactant monomers which can rapidly adsorb on the fiber surfaces.

In this study, the effect of micellar lifetime on the wetting time of cotton and rayon fabric in SDS solutions has been studied by measuring the wetting time and relaxation time (τ_2) of micelles as a function of surfactant concentration.

4.2 Experimental Procedure

A fabric of 1 in^2 was placed on the surface of SDS solutions at 25 °C. The surfactant solution displaces air in the textile surface by a wetting process and when sufficient air has been displaced, the textile starts sinking. The residence time of fabrics on the surface of the solution was measured as wetting time in this study. The wetting time in each SDS solution was measured four times. The average values are shown in figure 4-2 and 4-3.

4.3 Results and Discussion

All solutions of SDS were prepared above the CMC which is reported to be 8.2 mM,[86] since the main objective of this study was to determine the effect of micellar lifetime or stability on the wetting time of textile.

The wetting time of fabric in the SDS solutions was measured at various concentrations. According to equation (4.2), the adhesion tension (i.e.$\gamma_{L1L2}\cos\theta$) determines the penetrating power of solution into the inter-fiber spaces when the viscosity of solution η_1 is constant.

From Young's equation,

$$d(\gamma_{L_1L_2}\cos\theta) = -d(\gamma_{SL_2}) - d(\gamma_{SL_1}) \tag{4.3}$$

But the interfacial tension at the air/cotton interface (γ_{SL2}) is constant. Thus,

$$\frac{d(\gamma_{L_1L_2}\cos\theta)}{d(\gamma_{SL_1})} = -1 \tag{4.4}$$

The adhesion tension (i.e. wetting power) increases as the interfacial tension at the solution/cotton interface decreases.[87]

When the surfactant monomers are supplied rapidly to the wetting front of the

solution by the micellar disintegration, the interfacial tensions at air/solution and cotton/solution are decreased. But the adhesion tension of solution increases according to equation (4.4), because the change in $\cos\theta$ term is dominant as compared to γ_{L1L2}.

The monomers can be supplied rapidly to the wetting front by the micellar breakdown in unstable micellar solution compared to stable micellar solution. Therefore, wetting time is shorter in unstable micellar solution than in stable micellar solution.

The maximum wetting time occurred at 200 mM SDS concentration, at which most stable micelles are formed (Figures 4-2 and 4-3). Textile wetting depends upon effective reduction of the surface tension under dynamic conditions, i.e., as the wetting liquid spreads over the textile, the surface-active molecules must be supplied rapidly to the moving boundary between the liquid and the textile. The interfacial tension of textile/solution interface is determined by the concentration of surfactant monomers in the solution. The average monomer concentration is higher when micelles are relatively unstable. Micellar stability influences the wetting kinetics because higher monomer concentrations yield higher flux of surfactant monomers from the bulk to the wetting front and hence the adsorption to the textile surface.

In summary, the textile wetting time in sodium dodecyl sulfate solution was

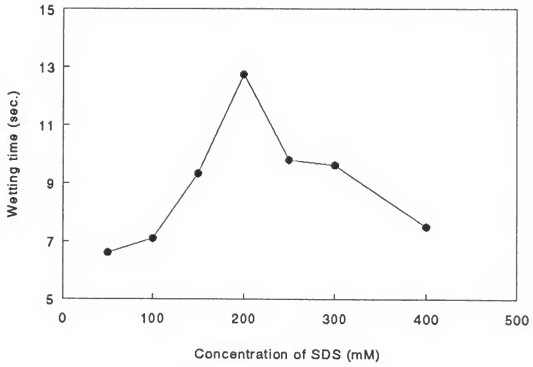

Figure 4-2 The effects of micellar relaxation time (τ_2) on the wetting time of cotton in SDS solution at 25 °C.

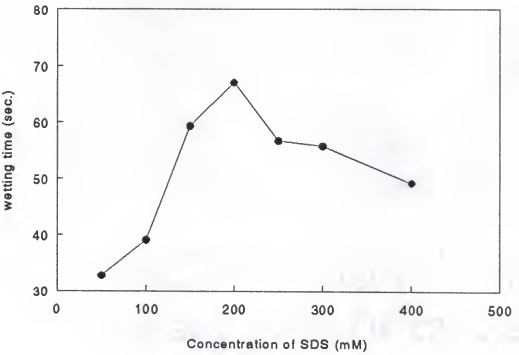

Figure 4-3 The effects of micellar relaxation time (τ_2) on the wetting time of rayon in SDS solution at 25 °C.

significantly influenced by the micellar lifetime which determines the monomer flux to the wetting front in surfactant solution. The wetting time of textile as well as the micellar stability as inferred from the relaxation time were maximum at 200 mM of SDS concentration.

CHAPTER 5
THE EFFECT OF MICELLAR LIFETIME ON EMULSION DROPLET SIZE

5.1 Introduction

Emulsions have been defined as heterogenous systems of one liquid dispersed in another in the form of droplets usually exceeding 0.1 μm in diameter, and each droplet is coated with a monolayer of the surfactant or emulsifier molecules. The two liquids are generally immiscible, chemically unreactive, and form systems characterized by a thermodynamic instability.[88] Research about formation, stability and characteristics of emulsions have been done extensively due to their wide application such as paints, polishes, pesticides, metal cutting oils, food, cosmetics textile processing and polymerization.[89,90]

Emulsions may consist of droplets of oil in water (o/w) or water in oil (w/o), depending upon water:oil ratio, emulsifier structure and concentration, temperature, addition of electrolyte and pressure. The structure of an emulsion (e.g., oil-in-water or water-in-oil) can be determined by electrical conductivity measurement, dilution of the emulsion in water or oil, viscosity variation with added oil or water and dye-

uptake methods.[17]

During emulsion formation, the surfactant molecules adsorb at the oil/water interface from the solution. The surfactant film decreases the interfacial tension, forms a barrier delaying the coalescence of the droplets by changing steric, viscous and elastic properties of the interface and provides the electrostatic charge to the droplets.[12]

An emulsification process needs energy to disperse one liquid into a continuous phase as droplets (Figure 5-1). The interfacial area is dramatically increased during this dispersion process. The work required (W) to expand the interfacial area is given by;[91]

$$W = \gamma \cdot (\Delta A) \qquad (5.1)$$

where γ is the interfacial tension and ΔA is the increase in the interfacial area. For constant W, a higher value of γ yields smaller ΔA. Thus, emulsion droplet size increases as the interfacial tension increases. The interfacial tension between oil/water during the emulsification process is determined by the effectiveness of the surfactant monomers to adsorb at the interface from the bulk solution (from water phase for o/w emulsion, from oil phase for w/o emulsion). The rate of surfactant monomer adsorption from the bulk to the interface is determined by the following

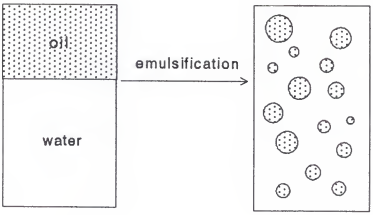

Figure 5-1 Emulsification process in the oil/water mixture.

processes: (i) rate of adsorption and desorption at the interface, (ii) rate of diffusion of monomers from the bulk to the oil/water interface,[92] and (iii) augmentation of flux of surfactant monomers due to the disintegration of micelles. In this study, it is proposed that short-lived micelles (i.e., small relaxation time) can effectively augment the flux of monomers from the bulk to the oil/water interface in the solution.

Therefore, the adsorption of surfactant monomers at the oil/water interface is influenced by the rate of disintegration of micelles (Figure 5-2). The dynamic interfacial tension at the oil/surfactant solution interface will be higher when micelles are relatively stable (i.e., long relaxation time). Higher dynamic interfacial tension results in smaller ΔA and hence larger droplet size. Systematic research about the effect of this micellar lifetime on emulsion droplet size has not been studied previously.

In this study, the effect of lifetime of micelles on the emulsion droplet size of hexadecane/aqueous sodium dodecyl sulfate (SDS) solution and hexadecane/aqueous cesium dodecyl sulfate (CsDS) solution has been investigated by the pressure-jump technique for micellar relaxation time (τ_2) and optical microscope for the droplet size.

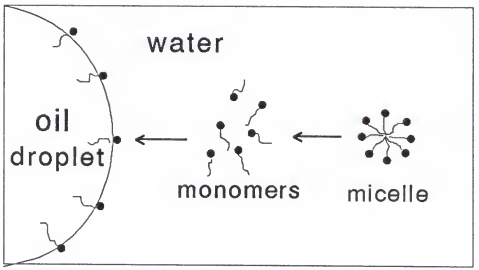

Figure 5-2 Schematic diagram for the adsorption of surfactant monomers from the bulk to the oil/water interface during the emulsion formation.

5.2 Experimental Procedure

The relaxation time of SDS solution saturated with hexadecane (Fisher Chemical, 99%) was also measured to study the effect of hexadecane on the micellar lifetime. Hexadecane was added into SDS solutions and shaken for 30 minutes to bring the mixture to equilibrium state. The shaken mixtures were centrifuged at 4000 rpm for 10 minutes to remove the foams generated during the mixing. CsDS, synthesized according to literature,[93] was also employed to make emulsions using the same procedure as mentioned above. The 4 ml of hexadecane was added into the 20 ml of micellar solutions of various surfactant concentrations (50, 100, 200, 300 and 400 mM of SDS concentration and 50, 75, 100, 150 mM of CsDS concentration), and vigorously shaken by a vibrator for 30 seconds at constant frequency of vibration to make emulsions. The hexadecane/SDS solution mixtures of same concentration as before were made separately, and emulsified for 1 minute. The pictures of emulsion droplets were taken through the optical microscope (Nikon, Japan) at 400 magnification just after the formation of emulsions to avoid coalescence or flocculation of droplets.

5.3 Results and Discussion

The relaxation time of SDS solutions saturated with hexadecane was the same

as those of pure SDS solutions, suggesting an insignificant solubilization of hexadecane in SDS solution (less than 4 μg per 100 ml SDS solution in experimental range of concentration).

Figure 5-3 shows the droplet size of emulsions of hexadecane/SDS solutions of various concentrations. The emulsion droplet size also increased as the concentration of SDS increased up to 200 mM SDS concentration, and then decreased with SDS concentration. The droplet size was maximum at 200 mM of SDS concentration at which the most stable micelles are formed. This is due to the minimum flux of monomers to the newly generated oil/water interface during the emulsification process. Because micelles are most stable at 200 mM SDS concentration, they cannot effectively augment the flux of monomers by their disintegration. The dynamic interfacial tension at the oil/solution interface of hexadecane/200 mM SDS solution will be maximum due to the minimum flux of monomers from the bulk to the interface. Therefore, the largest droplet size is produced at 200 mM concentration of SDS when the same amount of work is applied to the mixtures.

Figure 5-4 shows the droplet size of the emulsion of hexadecane/SDS solutions after 1 minute of emulsification. In this case, the droplet size of the emulsion was almost the same at all SDS concentrations probably due to larger input of energy and longer emulsification time which would allow the disintegration of micelles and subsequent adsorption of surfactant monomers at the oil/water interface.

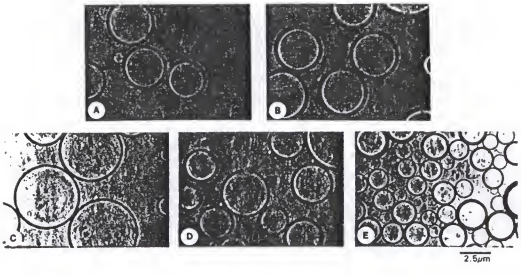

Figure 5-3 The emulsion droplet size in the mixture of hexadecane/SDS solutions after 30 seconds emulsification. (A) at 50 mM, (B) at 100 mM, (C) at 200 mM, (D) at 300 mM and (E) at 400 mM SDS solution.

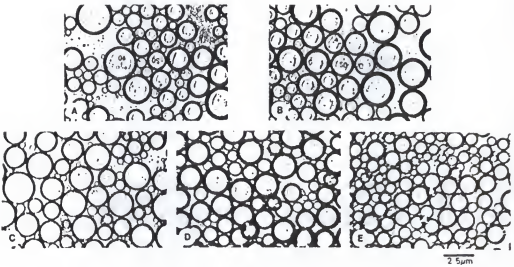

Figure 5-4 The emulsion droplet size in the mixture of hexadecane/SDS solutions after 1 minute emulsification. (A) at 50 mM, (B) at 100 mM, (C) at 200 mM, (D) at 300 mM and (E) at 400 mM SDS solution.

Thus, it appears that the stability of micelles may not exert influence on the droplet size if the emulsification is continued for a long time.

Figure 5-5 shows the droplet size of an emulsion of hexadecane/CsDS solutions after 30 seconds emulsification. The droplet size of emulsion was maximum at 100 mM CsDS concentration at which the most stable micelles were formed.

The previous chapters on foamability and bubble dynamics in SDS solutions showed the minimum foamability and minimum rate of bubble generation at 200 mM SDS concentration due to a decrease in the flux of monomers. It has also been discussed that the wetting time or penetration time of various fabrics in SDS solutions is maximum at 200 mM SDS concentration. The correlation between micellar lifetime and droplet size in emulsions raises some important implications for emulsion science in general.

In conclusion, the stable micelles of surfactants cannot augment the flux of surfactant monomers to the newly generated oil/solution interface during the emulsification process. The emulsion droplet size was found to be maximum for 200 mM SDS and 100 mM CsDS solutions with hexadecane due to the above-mentioned mechanism. Micellar lifetime was also maximum at the same concentration of SDS and CsDS.

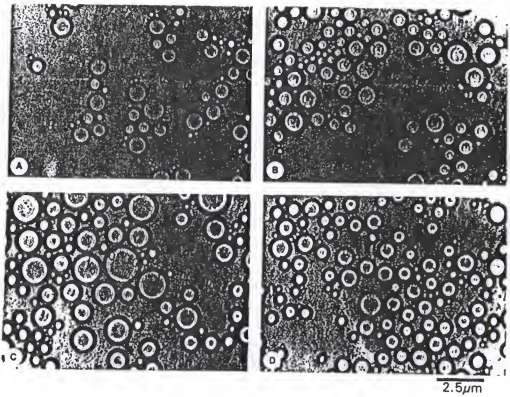

Figure 5-5 The emulsion droplet size in the mixture of hexadecane/CsDS solutions after 30 seconds emulsification. (A) at 50 mM, (B) at 75 mM, (C) at 100 mM and (D) at 150 mM CsDS solution.

CHAPTER 6
THE EFFECT OF COUNTERION SIZE ON THE INTERFACIAL TENSION AND EMULSION DROPLET SIZE IN DODECYL SULFATE AND HEXADECANE SYSTEMS

6.1 Introduction

The ionic surfactants dissociate into ionic surface active molecules and counterions when they are dissolved in the water. These counterions significantly influence the properties of surfactant solutions, e.g., CMC (critical micelle concentration), micellar size, micellar catalytic activity, etc. The CMC in aqueous solution reflects the degree of binding of the counterion to the micelle. For aqueous systems, the increased binding of the counterions to surfactants causes a decrease in the CMC of the surfactant. The extent of binding of the counterion increases with increase in the polarizability and valence of counterions, and decreases with increase in its hydrated radius.[17] Thus, in aqueous solution, for the anionic dodecyl sulfate, the CMC decreases in the order $Li^+ > Na^+ > Cs^+$. The CMC of LiDS, NaDS and CsDS were reported to be 8.92, 8.32 and 6.09 mM at 25°C by the measurement of specific conductance of solutions.[94]

Missel, et al.[95] have reported that the micellar size is in the following order: R_h(CsDS) > R_h(NaDS) > R_h(LiDS) at a given ionic strength, detergent concentration, and temperature. In general, the micellar catalysis is inhibited by counterions and the larger the counterion, the greater is the effect.[96] Also the ionized counterions perturb the local ordering or 'structure' of water molecules. Several water molecules are bound to counterions due to ion-dipole interaction between counterions and water molecules.[97]

As shown in table 6-1, the non-hydrated ion size follows the order of Li^+ <Na^+ <Cs^+, but the hydrated ion size come in reverse order due to the greater hydration of a lithium ion compared to a sodium or cesium ion. The diffusion coefficient of lithium ion in water is minimum due to largest hydrated ion size as shown in table 6-2.[98] The repulsive force between similar hydrated ions appears to increase on going from K^+-K^+ to Na^+-Na^+ to Li^+-Li^+ (rather than the opposite as would be expected from the non-hydrated ion radii of these ions).[97] Therefore, the effectiveness of monovalent cations as coagulants decreases according to the so-called lyotropic series, viz., Cs^+ > K^+ > Na^+ > Li^+ for monovalent ions.[99] The surface tension of surfactant solutions depends on the number of surfactant molecules at the surface. For a given surfactant, the greater concentration of surfactant molecules at the surface results in the lower surface tension.

In this study, the effect of the size of counterions of anionic dodecyl sulfate

Table 6-1. The values for the non-hydrated ion radius, hydrated ion radius, solvated layer thickness and solvation volume of each ion.

	Non-hydrated ion radius (nm)	Hydrated radius (nm)	Solvation layer thickness (nm)	Solvation volume (nm^3)
Li^+	0.068	0.38	0.312	0.230
Na^+	0.095	0.36	0.265	0.195
K^+	0.133	0.33	0.197	0.150
Cs^+	0.169	0.33	0.161	0.150

Table 6-2. Ionic diffusion coefficients (D_i) in water at 25 °C.

Cation	D_i (x 10^{-5} cm^2/sec.)
Li^+	1.03
Na^+	1.33
K^+	1.96
Cs^+	2.06

on the surface tension, interfacial tension at the hexadecane/water interface and the emulsion droplet size of hexadecane and water mixtures were investigated. The surfactants studied are lithium dodecyl sulfate (LiDS), sodium dodecyl sulfate (NaDS) and cesium dodecyl sulfate (CsDS). Potassium dodecyl sulfate (KDS) was not studied because micelles can not be formed at 25 °C due to its higher Krafft point (~30 °C).

6.2 Foam Fractionation of Surfactant Solutions to Remove Trace Impurities

Foam fractionation offers a useful technique for concentrating and separating solutes of differing degrees of surface activity. LiDS (Kodak Company, 95%), NaDS (Sigma Company, 99%) and CsDS (synthesized according to literature[93]) were purified by foam fractionation method before use. When a surfactant exhibits a minimum in surface or interfacial tension, it is primarily due to trace impurities in the surfactant.[100] The removal of such impurities eliminates the minimum in surface or interfacial tension. The foam fractionation is one of the most efficient method to remove the surface active impurities from the surfactants. The trace impurities in the surfactant (e.g., dodecanol) partition in the foam when foam is generated in the solution due to higher surface activity of dodecanol compared to that of C_{12} sulfate.[35]

Air was blown into the surfactant solutions of 25 mM concentration in the

column to make foam. Then the bottom solution was taken into another foam column. This procedure was repeated three times for each surfactant. 10 ml of solution was taken into the beaker after foam fraction. The water in the beaker was completely dried in the oven at 90 °C for 24 hours to obtain the amount of surfactant in 10 ml of solution after foam fraction as recommended.[101]

6.3 Experimental Procedure

The surface tension of LiDS, NaDS and CsDS solutions was measured by Rosano surface tensiometer (Biolar Corporation) using Wilhelmy plate method. Double-distilled water was used to prepare surfactant solutions. Also the interfacial tension between hexadecane and surfactant solutions was measured by the Wilhelmy plate method.

The 4 ml of hexadecane was added into the 20 ml of surfactant solution of various concentrations, and vigorously shaken by vibrator for 30 seconds at a constant frequency of vibration to make emulsion. The photographs of emulsion droplets were taken through the optical microscope (Nikon, Japan) at 400 magnification just after the formation of emulsions to avoid the coalescence or flocculation of droplets.

6.4 Results and Discussion

As shown in figure 6-1, the surface tension of LiDS solution is higher than that of NaDS or CsDS solution. There was no surface tension minima near the CMC after foam fraction of surfactant. The interfacial tension between hexadecane and LiDS solution was higher than that between hexadecane and NaDS or CsDS solution (Figure 6-2).

This can be explained as follows. The area/molecule at interface of LiDS is larger than that of NaDS or CsDS molecules due to larger size of hydrated counterions bound to the surfactant molecule as shown in table 6-1. The area/molecule at the interface can be calculated using the Gibbs adsorption isotherm.[85]

$$d\gamma = -\Sigma \Gamma_i d\mu_i \qquad (6.1)$$

where $d\gamma$ = the change in surface or interfacial tension of the solution

Γ_i = the surface excess concentration of component i

$d\mu_i$ = the change in chemical potential of component i in the solution.

At equilibrium between the interfacial and bulk phase, $d\mu_i = RTd\ln a_i$, where a_i is the activity coefficient of component i in the bulk phase, R is the gas constant, and T is

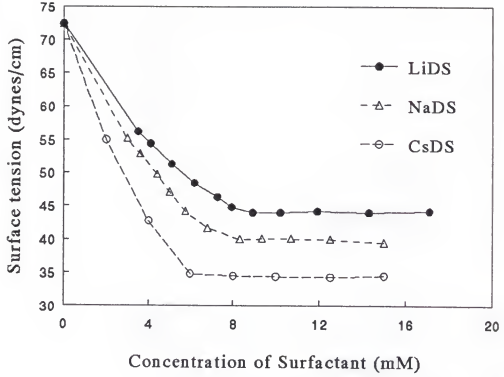

Figure 6-1 The surface tension of dodecyl sulfates with different counterions at air/water interface after foam fraction at 25 °C.

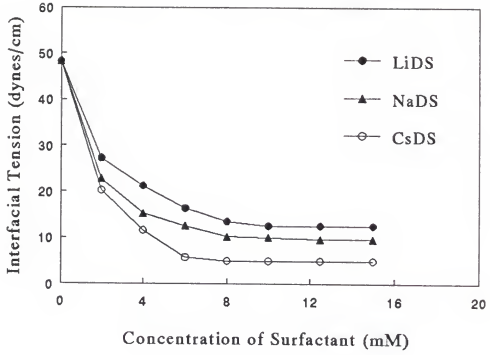

Figure 6-2 The interfacial tension of dodecyl sulfates with different counterions measured by Wilhelmy Plate method at the hexadecane/water interface.

the absolute temperature. Thus,

$$d\gamma = -RT\Sigma\Gamma_i d\ln a_i \tag{6.2}$$

$$= -RT\Sigma\Gamma_i d\ln x_i f_i \tag{6.3}$$

$$= -RT\Sigma\Gamma_i d(\ln x_i + \ln f_i) \tag{6.4}$$

where x_i is the mole fraction of component i in the bulk phase and f_i is its activity coefficient.

For solutions of a completely dissociated surfactant of the 1:1 electrolyte type, A^+B^-, as the only solute such as SDS, LDS and CsDS,[17]

$$d\gamma = -RT(\Gamma_A . d\ln a_A + \Gamma_B . d\ln a_B) \tag{6.5}$$

Since $\Gamma_{A+} = \Gamma_{B-} = \Gamma$ to maintain electroneutrality and $a_{A+} = a_{B-} = C \times f_i$ without significant error, then

$$d\gamma = -2RT\Gamma d(lnC + lnf_i) \tag{6.6}$$

where f_i is mean activity coefficient of the surfactant.

For dilute solutions, f_i can be approximated as one. Therefore, the Gibbs adsorption equation for ionic surfactants of 1:1 electrolyte type can be expressed as;

$$\Gamma = -\frac{1}{2RT}\frac{d\gamma}{dlnC} \tag{6.7}$$

The area/molecule at the interface can be calculated by dividing the film area by Γ. The area/molecule of each surfactant calculated by this equation at the air/water and oil/water interface is shown in table 6-3 and table 6-4. The area/molecule of LiDS was 61.3 $Å^2$ at the air/water interface compared to 51.8 for NaDS and 44.8 for CsDS. Also the area/molecule of LiDS at the oil/water interface was larger than that of NaDS or CsDS.

An emulsification process needs energy to disperse one liquid into another liquid as droplets. The interfacial area dramatically increases during the

Table 6-3. The area/molecule of dodecyl sulfate at the air/water interface and the surface tension above CMC.

	Area/molecule ($Å^2$/molecule)	Surface tension above CMC (dyn/cm)
LiDS	61.3	44.2
NaDS	51.8	40.0
CsDS	44.8	34.4

Table 6-4. The area/molecule of dodecyl sulfate at the hexadecane/water interface and the interfacial tension above CMC.

	Area/molecule ($Å^2$/molecule)	Interfacial tension above CMC (dyn/cm)	Average droplet size at 100 mM (μm)
LiDS	82.9	12.55	7
NaDS	68.9	9.65	5
CsDS	55.2	5.0	2.5

emulsification process. The work required (W) to expand the interfacial area is given by;[83]

$$W = \gamma \cdot (\Delta A) \tag{6.8}$$

where γ is the interfacial tension and ΔA is the increase in the interfacial area. For constant W, a higher value of γ yields smaller ΔA. Thus, the emulsion droplet size increases as the interfacial tension increases.

Figure 6-3 and 6-4 show the droplet size of emulsion of LiDS/hexadecane, NaDS/hexadecane and CsDS/hexadecane system at 50 and 100 mM surfactant concentration. The emulsion droplet size of hexadecane/LiDS system was larger than that of hexadecane/NaDS or hexadecane /CsDS system due to larger values of interfacial tension γ as explained in equation (6.8). The droplet sizes of emulsion at 50 mM surfactant concentration are smaller than those at 100 mM concentration. This is due to the effect of micellar lifetime. The lifetime of micelles at 100 mM is longer than that of 50 mM for each surfactant. The more stable micelles can not augment the flux of surfactant monomers to the rapidly expanding oil water interface during the emulsification process.

In conclusion, the number of LiDS molecules at the interface is less than that

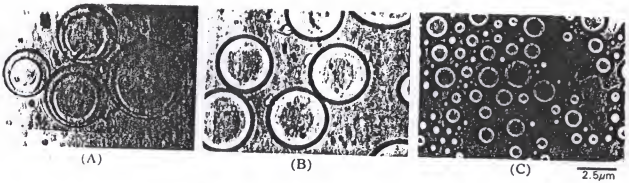

Figure 6-3 The emulsion droplet size in the mixture of hexadecane/50 mM surfactant solution. (A) LiDS, (B) NaDS and (C) CsDS.

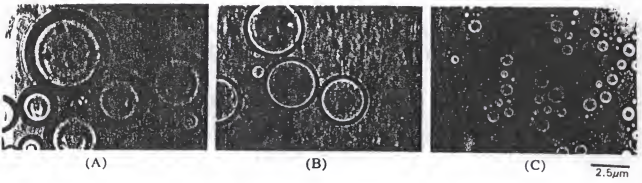

Figure 6-4 The emulsion droplet size in the mixture of hexadecane/100 mM surfactant solutions. (A) LiDS, (B) NaDS and (C) CsDS.

of NaDS and CsDS due to larger hydrated lithium ion. The largest hydrated counterion size of Li^+ in LiDS resulted in the highest surface tension of solution (Figure 6-1), the highest interfacial tension between hexadecane/water interface (Figure 6-2) and the largest emulsion droplet size of oil/water mixtures (Figures 6-3 and 6-4) compared to NaDS and CsDS surfactant.

CHAPTER 7
THE EFFECT OF MICELLAR LIFETIME ON THE RATE OF SOLUBILIZATION AND DETERGENCY IN SDS SOLUTIONS

7.1 Introduction

Solubilization is defined as the spontaneous formation of a thermodynamically stable isotropic solution of a substrate (the solubilizate), normally insoluble or only slightly soluble in a given solvent, by the addition of a surfactant.[102] Solubilization into the aqueous media is of a major practical importance in such areas as the formulation of products containing water-insoluble ingredients, where it can replace the use of organic solvents or cosolvents; in detergency, where solubilization is believed to be one of the major mechanisms involved in the removal of oily soil; in the separation of materials for manufacturing or analytical purposes. Solubilization into nonaqueous media is of major importance in dry- cleaning.[17] The solubilization of materials in biological systems sheds light on the mechanisms of the interaction of drugs and other pharmaceutical materials with lipid bilayers and membranes.[103]

The location in the micelle at which solubilization occurs varies with the nature of the materials solubilized and is of importance in that it reflects the type of

interaction occurring between surfactant and solubilizate. Solubilization is believed to occur at a number of different sites in the micelle: (1) on the surface of the micelle, at the micelle-solvent interface; (2) between the hydrophilic head groups; (3) in the so-called palisade layer of the micelle between the hydrophilic groups and the first few carbon atoms of the hydrophobic groups that comprise the outer core of the micellar interior; (4) more deeply in the palisade layer; and (5) in the inner core of the micelle.[12] These locus of solubilization are obtained mainly from studies on the solubilizate before and after solubilization, using X-ray diffraction,[104] UV spectroscopy[105] and NMR spectrometry.[106] Diffraction studies measure changes in micellar dimensions on solubilization, whereas UV and NMR spectra indicate changes in the environment of the solubilizate on solubilization.

Karaborni et al. performed molecular dynamic simulations on water/oil/surfactant system to mimic the solubilization mechanism of nonpolar molecules into aqueous micellar solutions.[107] They have identified three mechanisms in transferring of oil molecules from oil phase to the micelles: (1) dissolution of oil molecules in the solvent phase before being captured by micelles, (2) exchange of oil molecules between the oil droplet and the micelles during a soft collision and (3) collective desorption of surfactants and oil molecules from the oil droplet surface.

The amount of solubilizate that can be solubilized in the micellar solution depends on the structure of surfactant, structure of solubilizate, temperature and additives, etc.[102] Nonionic surfactants are better solubilizing agents than ionic in very

dilute solutions because of their lower critical micelle concentration.[108] For hydrocarbons and long-chain polar compounds that are solubilized in the interior of the micelle or deep in the palisade layer, the amount of material solubilized generally increase with increase in the size of micelles. Therefore, an increase in the chain length of the hydrophobic portion of the surfactant generally results in increased solubilization capacity for hydrocarbons.[109] Klevens[110] pointed out that in most cases increasing the length of the alkyl chain either in a straight-chain or substituted on a benzene ring decreases the solubility in a micellar solution, and that unsaturated compounds are more soluble than their saturated counterparts. In most cases the amount of solubilization increases with temperature due to the changes in the aqueous solubility properties of the solubilizates and changes in the properties of micelles.[111] For ionic micelles the addition of electrolyte causes an increases in micellar size and a decreases in the CMC. Therefore, the addition of electrolyte generally increases the amount of solubilization.[112]

The previous studies indicate that like the surfactant monomers, the solubilized molecules are not rigidly fixed in the micelle but have a freedom of motion which is dependent to some extent on the solubilization site.[113] The residence time of benzene molecules in SDS micelles was measured by analyzing the NMR signal of SDS solutions saturated with benzene. However, the lifetime of the solubilized molecule within the micelles was too short to be determined by this technique, but was thought to be not longer than 10^{-4} second. The other studies

showed that the lifetime of t-butyl-(1,1-dimethylpentyl)-nitroxide in SDS micelles was $3.3x10^{-6}$ second by electron spin resonance.[114] Also the lifetime of solubilizate in micelles increases with the increase of hydrocarbon chain length in sodium octyl, decyl and tetradecyl sulfate solutions.

Even though the equilibrium properties of solubilization in micellar solution such as the maximum amount of solubilizate which can be solubilized in a given surfactant solution and the loci of solubilizate in the micelle have been studied extensively, the kinetics of solubilization has not been clearly understood. Chan et al. proposed a theory of solubilization kinetics and its relation to the flow of dissolution medium, based on an analysis of five steps. Surfactant molecules diffuse to the surface as micellar species (step 1). These molecules are adsorbed on the surface of solubilizate (step 2) and on the surface the surfactant and solubilizate form a mixed micelles (step 3). In step 4, the mixed micelles are dissolved and they diffuse away into bulk solution (step 5). But there is no proof that micelles diffuse to the surface and adsorb in this model.[115]

In this study, the effect of micellar lifetime on the rate of solubilization and detergency in SDS solutions was investigated by measuring the rate of movement of the interface between benzene and SDS solution, the rate of change in electrical conductivity after adding benzene into SDS solution, and the rate of dye-removal from cotton to SDS solution.

7.2 Experimental Procedure

7.2.1 The rate of movement of the benzene/surfactant solution interface:

5 ml of benzene (Fisher Chemical Co., 99 %) was added into 50 ml of SDS solution in the flask (Figure 7-1). The SDS solution in the bottom was agitated gently by magnetic stirrer, and the rate of upward movement of the interface was measured.

7.2.2 The rate of solubilization of benzene by electrical conductivity method:

The electrical conductivity of 50 ml of SDS solution was measured by conductivity bridge (YSI model 31) until there is no change of conductivity while stirring, indicating that the system has reached the equilibrium state at the ambient condition. 1 ml of benzene was added into the 50 ml of SDS solution. The electrical conductivity of the benzene/SDS solution mixture was measured as a function of time. If there is no more change in conductivity with time, we considered that time as the time required to solubilize benzene into SDS solution up to its saturation limit.

7.2.3 The rate of detergency of Orange OT adsorbed on cotton by SDS solutions:

Orange OT (0.05 gram) was dissolved into 5 ml of benzene, 0.4 ml of this dye solution was applied to cotton pieces of 5"x5". The benzene was removed from

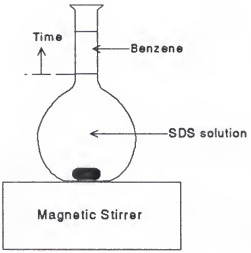

Figure 7-1 The experimental set-up for the measurement of the rate of movement of the benzene/SDS solution interface by stirring.

cotton by drying. The cotton pieces were submerged into 250 ml of SDS solution in Tergotometer. Tergotometer was operated at 25 °C. A small amount of surfactant solution (3 ml) was withdrawn from Tergotometer at different to measure the absorbance of light at 505 nm to measure the concentration of Orange OT.

7.3 Results and Discussion

Figure 7-2 shows the rate of upward displacement of interface between benzene and SDS solutions. The rate was maximum at 200 mM concentration at which most stable micelles are formed. Figures 7-3, 7-4 and 7-5 show the electrical conductivity change after adding the benzene into SDS solution at 100, 200 and 300 mM concentration. The electrical conductivity of mixtures at other concentrations also decay in a similar way, but it took longer time to reach equilibrium than at 200 mM SDS concentration. The decay curve of conductivity can be used as a measure of the rate of solubilization because the solubilization of benzene decreases the CMC and hence monomer concentration.[116] This results in a decrease of electrical conductivity. The electrical conductivity of the mixture of benzene and SDS solution reaches the equilibrium value in the minimum time for 200 mM SDS concentration. This indicates that the highest rate of solubilization of benzene into SDS solutions occurred at 200 mM SDS concentration (Figure 7-6).

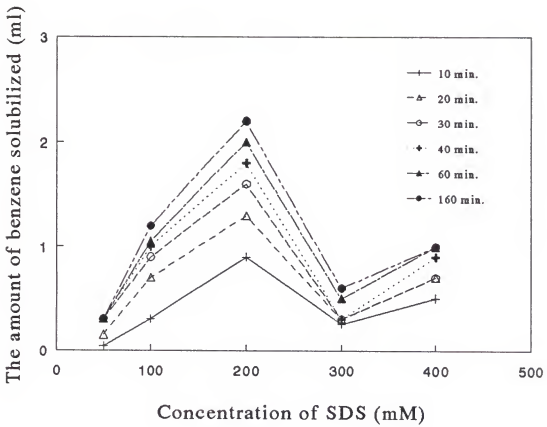

Figure 7-2 The amount of benzene solubilized into SDS solutions at various time intervals measured by the rate of interface movement.

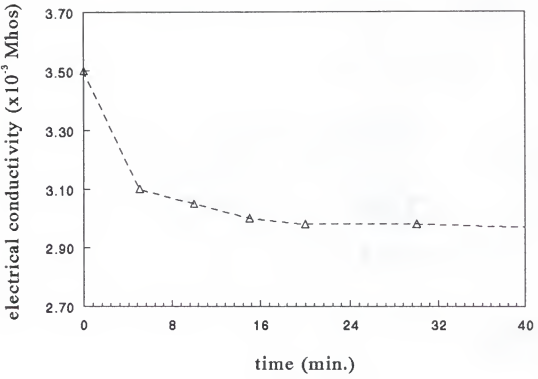

Figure 7-3 The electrical conductivity change of solution after adding benzene into SDS solution at 100 mM concentration.

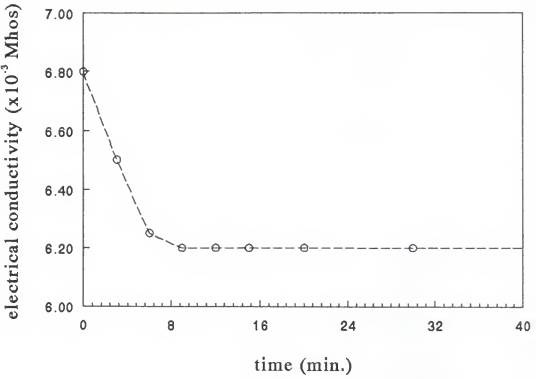

Figure 7-4 The electrical conductivity change of solution after adding benzene into SDS solution at 200 mM concentration.

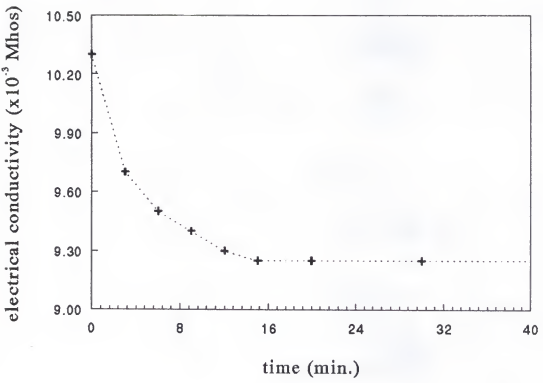

Figure 7-5 The electrical conductivity change of solution after adding benzene into SDS solution at 300 mM concentration.

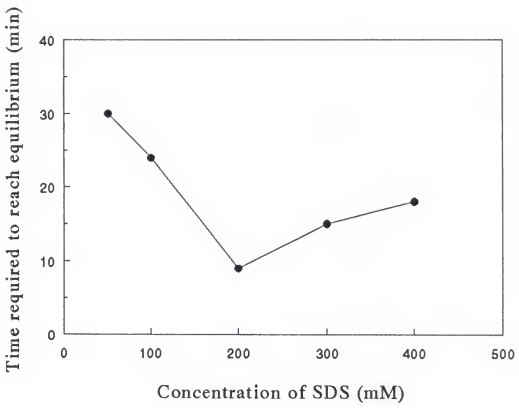

Figure 7-6 The time required to solubilize 1 ml of benzene into 50 ml of SDS solutions using electrical conductivity method.

In detergency, solubilization of soil from fabric into the detergent solution is one of most important events. The rate of dye (Orange OT) removal from cotton to SDS solutions in Tergotometer was maximum at 200 mM concentration (Figure 7-7).

The micelles become more and more rigid and stable as the SDS concentration increases up to 200 mM due to coulombic repulsion between them. The interior of rigid (i.e. tightly packed) micelles becomes more and more hydrophobic compared to that of the loosely packed micelles. The stronger hydrophobic core of the rigid micelles causes the rapid solubilization of benzene and Orange OT into the micelles at 200 mM SDS concentration.

In conclusion, the relatively more stable micelles (longer relaxation time, τ_2) are formed at 200 mM SDS concentration at 25°C, and the rate of solubilization of benzene and Orange OT into SDS micelles is maximum at 200 mM concentration. Therefore, we conclude that more stable micelles are more favorable for solubilization and detergency.

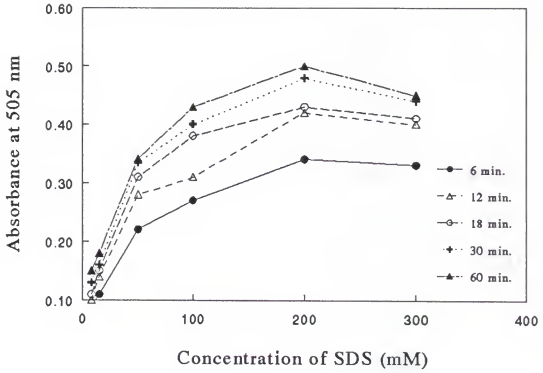

Figure 7-7 The rate of solubilization of Orange OT from cotton into SDS solution in the Tergotometer.

CHAPTER 8
MODELLING ON THE RATE OF CHANGE IN MONOMER CONCENTRATION AT THE SURFACE

8.1 Introduction

Most of the dynamic behaviors described in the previous chapters are related to the rate of change in the monomer concentration at the newly created surface.[117,118] The rate of change of surface concentration of monomers is governed by the slowest process of following three processes; (1) breakdown of micelles, (2) diffusion of surfactant monomers from the bulk to the surface and (3) adsorption/desorption of monomers at the surface.[92] In case of organic surfactants, adsorption/desorption kinetics are known to be much faster unless the monomer concentration in the bulk is very low. In the present system, the surfactant concentration in the bulk is very high. However, most of them are present in the form of micelles, and the monomer concentration is at equal to the CMC. When new surfaces are created during the dynamic process, it is likely that monomers in the bulk may be depleted unless they are supplied by the fast breakdown of micelles. Due to the very large slow relaxation time (τ_2) of SDS at high concentrations, such

conditions may not be created and the monomer concentration in the bulk will be low. Consequently, the adsorption/desorption at the surface will be always faster than bulk diffusion or breakdown of micelles. Thus, in the present modelling, the focus is given to examining the balance between bulk diffusion and micellar breakdown.

The first concept on the physical process of surfactant monomer adsorption was introduced by Milner.[119] Ward and Tordai made the first general model for a diffusion controlled adsorption.[120] Besides the model of diffusion controlled adsorption, models of kinetics and mixed diffusion-kinetic controlled adsorption were formulated and algorithm for their solution given.[121,122] Sutherland has derived mathematical expression for the concentration of surfactant monomers at surface as a function of time in absence of micelles in solution.[124] For the first time Miller discussed about the importance of micellar lifetime in the adsorption kinetics of surfactant monomers, and found that micellar lifetime plays a decisive role in determining the rate of adsorption of monomers from the bulk to the interface in a model system.[123]

In this chapter, mathematical simulation has been performed to study the effect of micellar lifetime on the adsorption kinetics in a real system (i.e., SDS solutions) using Miller's procedure.

8.2 Mathematical Description

The description of adsorption kinetics from micellar solution is usually based on a mathematical model in which the second Fickian law of diffusion is used for the transport of surfactant monomers and micelles, respectively:[125]

$$\frac{\partial c_1}{\partial t} = D_1 \frac{\partial^2 c_1}{\partial x^2} + q_1, \qquad x>0, \quad t>0 \tag{8.1}$$

$$\frac{\partial c_n}{\partial t} = D_n \frac{\partial^2 c_n}{\partial x^2} + q_n, \qquad x>0, \quad t>0 \tag{8.2}$$

where c_1 is the concentration of surfactant monomer, c_n is the concentration of micelles. D_1 and D_n are the diffusion coefficients of monomers and micelles. Also q_1 and q_n represent the rate of formation of surfactant monomers and micelles by the micellar kinetics.

The boundary and initial conditions are in analogy to the classical models:
i) at the interface

$$\frac{\partial \Gamma_1}{\partial t} = D_1 \frac{\partial c_1}{\partial x} \tag{8.3}$$

where γ_1 denotes the concentration of surfactant monomers at the interface.

$$\frac{\partial c_n}{\partial x} = 0, \quad x = 0 \tag{8.4}$$

(i.e., no adsorption of micelles at surface)

ii) in the bulk phase

$$c_i = c_{io}, \quad i = 1, n, \quad x = \infty \tag{8.5}$$

where c_{io} is the bulk concentration of i at equilibrium.

iii) at t = 0 there is a homogeneous distribution of monomers and micelles in the bulk

$$c_i = c_{io}, \quad 0 < x < \infty, \quad t = 0, \quad i = 1, \quad n \tag{8.6}$$

iv) no adsorption at the interface at t = 0 occurs

$$\gamma_1 = 0, \quad t = 0 \tag{8.7}$$

The generation term q1 and q_n in equations (8.1) and (8.2) are determined by the mechanism of micelle formation and micelle dissociation. There are different models describing micelle kinetics, but here the formation-dissociation mechanism according to Lucassen is used:[126]

$$n \cdot S \rightleftharpoons S_n \tag{8.8}$$

where n is the aggregation number of micelles, S and S_n represent the monomer and micelle, respectively.

Taking this mechanism as a basis, the relations for the generation follow:

$$q_1 = -nk_f c_1^n + nk_d c_n \tag{8.9}$$

$$q_n = k_f c_1^n - k_d c_n \tag{8.10}$$

where k_f and k_d denote the rate constants of micelle formation and micelle dissociation.

Using this model, the real distribution of monomers, premicellar aggregate, and micelles shown in figure 8-1 is displayed by an idealized distribution consisting of monomers and micelles only with the concentrations c_1 and c_n respectively. The effect of this idealization of the distribution of aggregate on micellar kinetics is negligible.

Since an analytical solution of this problem is impossible if the boundary and initial conditions are maintained. Therefore, it is useful to transform all relations into a dimensionless form by introducing the following parameters;[123]

$X = x/m_1$, $T = D_1 t/m_1^2$, $C_1 = c_1/c_{1o}$

$C_n = c_n/c_{no}$ (8.11)

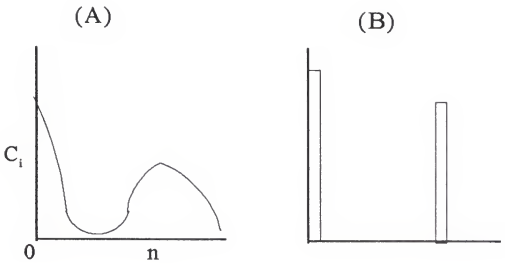

Figure 8-1 Distribution of aggregates in micellar solution (A) and idealized distribution of aggregates (B) in micellar solution.

$\Gamma_1 = \gamma_1/\gamma_{1o}$, $m_1 = \gamma_{1o}/c_{1o}$

$\alpha_1 = D_n/D_1$, $\alpha_2 = c_{no}/c_{1o}$, $\alpha_3 = nk_f c_{1o}^{n-1} m_1^2/D_1$

Then the following form of the boundary and initial value problem is obtained;

$$\frac{\partial C_1}{\partial T} = \frac{\partial^2 C_1}{\partial X^2} - \alpha_3 C_1^n + \alpha_3 C_n, \quad X>0, \quad T>0 \tag{8.12}$$

$$\frac{\partial C_n}{\partial T} = \alpha_1 \frac{\partial^2 C_n}{\partial X^2} + \frac{\alpha_3}{n\alpha_2} C_1^n - \frac{\alpha_3}{n\alpha_2} C_n, \quad X>0, \quad T>0 \tag{8.13}$$

$$\frac{\partial \Gamma_1}{\partial T} = \frac{\partial C_1}{\partial X}, \quad X=0, \quad T>0 \tag{8.14}$$

$$\frac{\partial C_n}{\partial X} = 0, \quad X=0, \quad T>0 \tag{8.15}$$

$$C_i = 1, \quad i=1, n, \quad T>0, \quad X=\infty \tag{8.16}$$

$$C_i = 1, \quad i=1,n, \quad X>0, \quad T=0 \tag{8.17}$$

$$\Gamma_1 = 0, \quad T = 0 \tag{8.18}$$

The additional relationship between Γ_1 and C_1 can be obtained by the Henry's adsorption isotherm,

$$\Gamma_1 = C_1, \quad X = 0 \tag{8.19}$$

This condition is equivalent to assuming that the adsorption/desorption process is so fast that local equilibrium is achieved instantly. As described section 8.1, this condition is plausible for the present situation.

Equation (8.14) can be rewritten as

$$\frac{\partial \Gamma_1}{\partial T} = \frac{\partial \Gamma_1}{\partial C_1} \frac{\partial C_1}{\partial T} = \frac{\partial C_1}{\partial X}, \quad X = 0, \quad T > 0 \tag{8.20}$$

From equation (8.19), we can get the following equation;

$$\frac{\partial \Gamma_1}{\partial C_1} = 1.0 \tag{8.21}$$

8.3 Finite Difference Method

To solve the problem numerically, a finite difference method was used. Equation (8.12) and (8.13) can be written by the following finite differential schemes.[127]

$$\frac{(C_1)_{i,j+1}-(C_1)_{i,j}}{(\Delta T)}=\frac{(C_1)_{i,j+1}-2(C_1)_{i,j}+(C_1)_{i,j-1}}{(\Delta X)^2}-\alpha_3[(C_1)_{i,j}^n-(C_n)_{i,j}] \tag{8.22}$$

$$\frac{(C_n)_{i,j+1}-(C_n)_{i,j}}{(\Delta T)}=\alpha_1\frac{(C_n)_{i,j+1}-2(C_n)_{i,j}+(C_n)_{i,j-1}}{(\Delta X)^2}+\frac{\alpha_3}{n\alpha_2}[(C_1)_{i,j}^n-(C_n)_{i,j}] \tag{8.23}$$

The equation (8.20) can be rewritten in the finite differential scheme,

$$(C_1)_{i,j+1}=\frac{\Delta T}{\Delta X}((C_1)_{2,j}-(C_1)_{1,j})+(C_1)_{1,j} \tag{8.24}$$

The step sizes were chosen as $\Delta T=0.01$ and $\Delta X=0.2$ to run the computer program. These step sizes satisfy the stability condition of program, which is that $(\Delta T)/(\Delta X^2)$

should be less than 0.5 .[127]

For high surfactant concentration, micellar relaxation time (τ_2) can be written as

$$\frac{1}{\tau_2} \approx k_r^- A_r \frac{n^2}{A_{tot}} \qquad (8.25)$$

where k_r^- and A_r are the rate constant of formation and concentration of least abundant aggregates in the distribution curve.[21] And k_r^- is equal to k_d, which is the dissociation rate constant of micelles. From equation (8.25) and (8.11), the values α_3 at different SDS concentrations can be calculated using slow relaxation time of micelles (τ_2).

Table 8-1 shows the values used in this calculation for α_1, α_2, α_3 and n at different SDS concentrations.

8.4 Results and Discussion

Figure 8-2 shows the surfactant monomer concentration at surface as a function of time in SDS solutions calculated using the program in appendix A. The concentration of surfactant monomers at surface, which determines the dynamic surface tension of solution,[128] was minimum at 200 mM SDS concentration. Therefore, the highest dynamic surface tension is expected at this

Table 8-1. The values of parameters used in computational calculation.

	at 100 mM	at 200 mM	at 300 mM
α_1	10^{-4}	10^{-4}	10^{-4}
α_2	0.195	0.391	0.313
α_3	0.2	0.0082	0.038
n	64	64	100

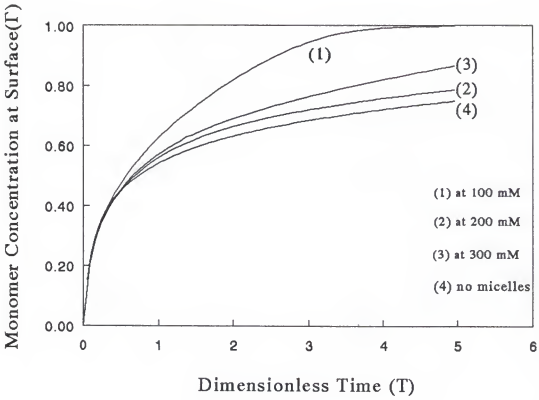

Figure 8-2 The SDS monomer concentration at surface as a function of time.

concentration. This highest dynamic surface tension at 200 mM SDS concentration resulted in the least foaming, the largest emulsion droplet size, the least frequency of bubble formation, largest bubble size and the longest textile wetting time.

CHAPTER 9
THE MOLECULAR MECHANISM FOR THE DESTABILIZATION OF FOAM BY ORGANIC IONS

9.1 Introduction

The effects of adding electrolyte to foams stabilized by ionic surfactants may be difficult to predict due to several counteracting mechanisms.[129] One contribution to the film stability is due to electrical repulsions between the ionic double layers associated with adsorbed ionic surfactants on the two sides of the liquid film. Since addition of electrolyte causes compression of the electrical double layers, it may decrease the stability of the foam. On the other hand, the presence of electrolyte reduces the repulsions between adjacent surfactant head-groups at the air/water interface, thus promoting the formation of more condensed films with higher surface viscosity. Hence, the latter mechanism is associated with an increase in the stability of the foam by electrolytes. A third mechanism that may be of importance is that the electrolyte affects the solubility of the surfactant. The concentration of surfactant may either be enhanced or reduced at the air/water interface when electrolyte is added.

The antifoaming mechanism of foam by foam breaker can be summarized as

follows;[17]

a) By removing surface active materials from the bubble surface:

The presence of certain types of soil in surfactant solution shows decreased foaming due to this mechanism because surfactant molecules are removed from the surface by adsorption onto or dissolution in the soil. Finely divided hydrophobic silica particles break the foam by adsorbing surfactant molecules from the bubble surface and carrying them into solution.

b) By replacing the foam-producing molecules with other molecules at the surface:

The surfactant molecules at the bubble surface are replaced by adding the rapidly diffusing noncohesive molecules of limited solubility in the solution. The tertiary acetylenic glycols, ethyl ether and isoamyl alcohol break foam in this manner.

c) By converting the surfactant film into solid brittle film with no elasticity:

Calcium salts of long chain fatty acids break foam in sodium dodecylbenzene sulfonate or sodium dodecyl sulfate solution by this mechanism.

d) By reducing the surface viscosity of the film:

Tributyl phosphate has a large cross sectional area at the air/water interface, and intercalate between surfactant molecules in the interfacial film. This

intercalation of surfactant molecules by tributyl phosphate molecules reduces the cohesive forces between them and consequently reduces the surface viscosity, followed by the increased drainage of liquid in the film.

The nature of the electrolyte is of course of importance in this context. Electrolytes containing multivalent metal ions can be anticipated to cause larger effects on the foam stability compared to those with monovalent ions, specially for ionic surfactants. Even when comparing the influence of a set of alkali metal chlorides, distinct differences in foam stabilities are observed.[130] In the present study, electrolytes containing organic ions have been investigated. A mechanism that is not common to inorganic electrolytes may be of importance here: larger organic ions adsorbed at the air/water interface may alter the packing of surfactant molecules and hence influence surface viscosities and foam stability.

In order to study the relationship between structure and foam inhibiting effects of organic ions, electrolytes containing tetraalkylammonium ions of different sizes have been investigated. A previous study concerning o/w emulsions has shown that tetraalkylammonium ions are very efficient demulsifiers,[131] which makes them interesting to study with regard to their antifoaming properties.

The foam destabilizing efficiency of the organic salts has been compared to

those of tributyl phosphate and 2-ethyl hexanol, which are wellknown antifoaming substances used in several commercial formulations. The reason why this comparison was made is that the foam inhibiting properties of tributyl phosphate and 2-ethyl hexanol have been attributed to their ability to reduce the surface viscosity of the foam films,[132,133] which is believed to be an important mechanism for the tetraalkylammonium salts.

9.2 Experiments

9.2.1 Materials

Surfactants

Sodium dodecyl sulfate, $C_{12}H_{25}OSO_3Na$, SDS, 99.9 %, Merck

Hexaethylene glycol ether, $C_{12}H_{25}(OCH_2CH_2)_6OH$, $C12E_6$, 99 %, Nikko Chemicals, Tokyo, Japan

Electrolytes, anti-foaming compounds

Tetramethylammonium bromide, TMAB, p s, Merck

Tetraethylammonium bromide, TEAB, p s, Merck

Tetrapropylammonium bromide, TPrAB, Fisher

Tetrabutylammonium bromide, TBAB, p s, Merck

Tetrapentylammonium bromide, TPAB, > 99 %, Aldrich Chemical company

Tetrabutylammonium chloride, TBAC, purum, Fluka AG

2-Ethyl hexanol, EH, p s, Merck

Tributyl Phosphate, TBP, p s, Merck

Sodium bromide, NaBr, p a, Merck

All chemicals were used as supplied.

9.2.2 Methods

The foam destabilizing efficiency of different additives were quantified by generating foam and measuring the half-life of the foam, $\tau_{1/2}$, corresponding to the time for the reduction of the foam volume to half of the initial volume. Two different methods were used to produce the foam. In the first method, the Ross-Miles set-up[134] was used to produce the foam. In a second method, the foaming solution (50 ml) was foamed at a constant gas flow rate (2.7 l/h) through a glass frit, in a 900 ml graduated cylinder. After 10 minutes of gas flow, the gas was turned off and $\tau_{1/2}$ was measured. If otherwise not stated, the second method was used in the experiments.

The $\tau_{1/2}$ values given in this paper correspond to average values of 3-5 independent experiments. The accuracy is estimated to be within 5 %. All measurements were carried out at 22-23 °C.

The surface tensions were measured by a de Noüy ring or Wilhelmy plate

method to calculate the area/molecule at the air/water interface and CMC of SDS in the presence of various organic salts.

The deep channel surface viscometer (as shown in Figure 9-1) was used to measure the surface shear viscosity of SDS solutions in the presence and absence of organic salts. The diameter of the inner channel wall is 9.21 cm, the diameter of the outer wall is 11.35 cm. The ratio of depth to width of the liquid channel (D) was chosen such that D always remained greater than $2/\pi$. For all experimental purposes a constant volume of the subphase was used and D was measured as 0.75 (channel width = 0.87 cm).

In the deep channel surface viscometer, the channel walls are stationary concentric cylinders; the floor of the viscometer moves with a constant angular velocity. It is important to note that in order to estimate the center-line velocity of the interface, the velocity of more than one particle carefully placed at the surface of the liquid in the annular channel needs to be measured.

The general assumptions in order to get an expression for surface shear viscosity at the air/water interface are;[135]

1. Both the liquid and the gas phases may be described as incompressible, Newtonian fluids.

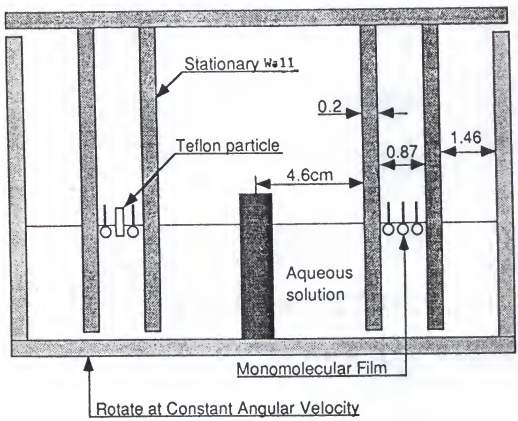

Figure 9-1 A schematic view of deep channel surface viscometer.

2. The interface is flat.

3. Any surfactant present is uniformly distributed over the interface.

4. There is no mass transfer across the interface.

With the above assumptions, for deep channels (i.e., $D > 2/\pi$), the fluid velocity at the fluid-fluid interface can be expressed as;[136]

$$V = \frac{8V_b}{\pi e^{\pi D}} \frac{\sin(\frac{\pi y}{y_o})}{1 + \frac{\pi e}{\eta y_o} + \frac{\eta^*(\tanh \pi D_1 + \frac{\epsilon^* \pi}{\eta y_o})}{\eta(1 + \frac{\epsilon \pi}{\eta y_o} \tanh \pi D_1)}} \qquad (9.1)$$

where η = bulk viscosity of the lower fluid

η^* = bulk viscosity of the upper fluid

y_o = channel width

V_b = plate rotational speed

ϵ = interfacial viscosity for the lower phase

ϵ^* = interfacial viscosity for the upper phase

The above expression can be further simplified for the air/water interface where η^* (the viscosity of the upper phase, i.e., air) can be considered as zero. By substituting $y = y_o/2$ for the center-line velocity and $\eta^* = 0$, the equation (9.1) can be simplified as;

$$V = \frac{8V_b}{\pi e^{\kappa D}} \quad \frac{1}{(1+\frac{\pi e}{\eta y_o})} \tag{9.2}$$

By rearranging equation (9.2), the final expression for the surface shear viscosity (ε) at the air/water interface can be described as;[137]

$$e = \frac{\eta y_o}{\pi}\left[\frac{8V_b}{\pi V e^{\kappa D}} - 1\right] \tag{9.3}$$

In order to measure the center-line velocity, a small Teflon particle was placed at the interface and the time for that particle to make one complete revolution under the certain plate angular velocity was recorded from visual observations. The problem often encountered while placing the particle at the interface, was the shift in radial position of the particle at the interface. This was mainly due to the difference in interfacial tension gradient developed in the immediate neighborhood of the particle

due to surface contamination.

For the measurement of surface viscosity, plate rotational speed was fixed at 4.6 rpm. Prior to selecting the rotational speed of 4.6 rpm, the linearity of the plate rpm versus particle rpm was checked at the air/water interface. The linearity of the result shown in figure 9-2 represented laminar flow of liquid at 4.6 rpm.

9.3 Results and Discussion

9.3.1 Symmetrical Tetraalkylammonium Bromide Salts

Table 9-1 shows the initial foam heights, as determined by the Ross-Miles procedure,[134] of foams stabilized by the anionic surfactant SDS in the presence of various electrolytes. Figure 9-3 displays the half-life, $\tau_{1/2}$, of these foams. The surfactant concentration is 14 mM, which is above the CMC of the pure surfactant (8 mM).

As may be seen from figure 9-3, the influence of NaBr on the foam stability was minor below a 1:1 ratio of NaBr/SDS. By contrast, drastic reductions in $\tau_{1/2}$ were observed even at small addition of electrolyte containing large tetraalkylammonium ions. The $\tau_{1/2}$ values are in the order TEAB > TBAB > TPAB. Hence, a correlation was observed between the size of the tetraalkylammonium ion and its destabilizing effect on the foam. Contrary to what was observed with regard to foam stability, the initial foam height was not significantly

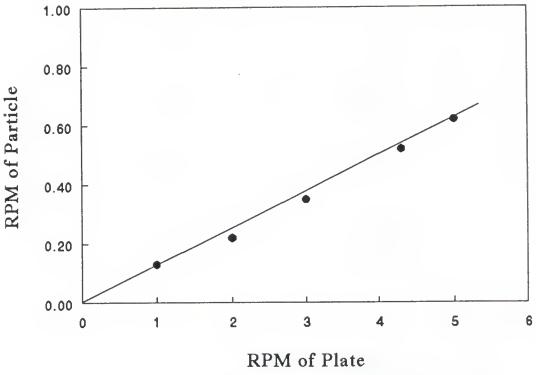

Figure 9-2 The rpm of teflon particle in deep channel surface viscometer in water solution without spreading any monolayer.

TABLE 9-1. Initial foam heights, obtained with the Ross-Miles method, of SDS in presence of different electrolytes. The foam heights are given for some different electrolyte/surfactant molar ratios (X).

Initial Foam Height							
$X_{NaBr/SDS}$	H, mm	$X_{TEAB/SDS}$	H, mm	$X_{TBAB/SDS}$	H, mm	$X_{TPAB/SDS}$	H, mm
0	180	0	180	0	180	0	180
0.19	170	0.11	180	0.11	172	0.11	160
1.00	175	0.28	172	0.23	170	0.29	147
2.11	175	0.47	175	0.46	175		
		0.69	175	0.66	172		

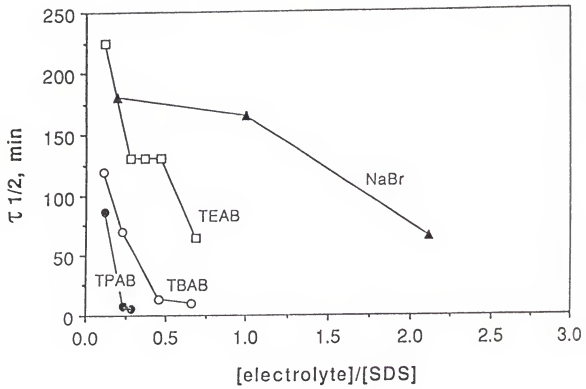

Figure 9-3 The half-life, $\tau_{1/2}$, of SDS foams in the presence of different electrolytes versus the electrolyte/SDS molar ratio. The electrolytes are tetrapentylammonium bromide (TPAB), tetrabutylammonium bromide (TBAB), tetraethylammonium bromide (TEAB) and NaBr. The SDS concentration was 14 mM. The foams were produced by the Ross-Miles procedure.

influenced by tetraalkylammonium bromide electrolytes. Only for TPAB could a substantial reduction in the initial foam volume be observed (Table 9-1).

There are several mechanisms that may be of importance in explaining the correlation between the size of the organic cations and the destabilizing effect on an ionic foam:

9.3.1.1 Reduced Electric Repulsions Between Surfactant Layers

From NMR self-diffusion measurements it is known that the attractive interactions between tetraalkylammonium ions and ionic surfactants increase with the size of the ion.[138] This is due to an increase in the hydrophobicity of the ions with the size of the alkyl chains. Hence, the surface potential, and therefore also electrical double layer repulsions which contributes to the foam stability, are lower in the presence of hydrophobic organic ions as compared to systems with less hydrophobic ions.

9.3.1.2 Reduced Surface Shear Viscosity

Qualitatively foam stability has been correlated with the surface viscosity of the adsorbed films. It is well accepted that if the surface viscosity is low, the foam produced will be unstable.[130,139-140] Shah et. al showed that the surface viscosity in mixed surfactant systems was maximum at the 1:3 molecular ratio due to the two-dimensional hexagonal arrangement of molecules at the interface. The maximum

surface viscosity at 1:3 molecular ratio produced the most stable foams.[38,42] The presence of large tetraalkylammonium ions at the air/water interface may perturb the packing of surfactants, producing noncoherent films with low surface viscosity and low stability. The surface shear viscosity of SDS (14 mM) solution in the presence of various salts (3 mM) decreased with an increase in the size of organic ions (Table 9-2). The lower surface viscosity in the presence of large organic ions will enhance the collapse of foam.

9.3.1.3 Reduced Surface Concentrations

The larger tetraalkylammonium ions form hydrophobic complexes with SDS molecules,[141] which may lead to an inactivation of the foam stabilizing ability of the surfactant. Specially, tetrapentylammonium ion made complexes with SDS molecules in our experimental concentration range. Therefore, the CMC of SDS in the presence of this ion could not be measured. The concentration of SDS at the air/water interface can be calculated from the following Gibbs adsorption equation.[85]

$$\Gamma = -\frac{1}{2RT}\frac{d\gamma}{dlnC} \tag{9.4}$$

The concentration of SDS at the air/water interface (Γ) was calculated using equation (9.4). The area/molecule of SDS at the air/water interface can be calculated dividing area by the surface concentration (Γ). The slope ($d\gamma/dlnC$) can

TABLE 9-2. The area/molecule of SDS and surface shear viscosity of the film when salt concentration is 3 mM and concentration of SDS is 14 mM.

	Area/Molecule ($Å^2$/molecule)	Surface Viscosity (cP)
In aqueous solution	51.8	0.11
$(CH_3)_4N^+$	110.6	0.06
$(CH_3CH_2)_4N^+$	118.3	0.054
$(CH_3CH_2CH_2)_4N^+$	133.0	0.049
$(CH_3CH_2CH_2CH_2)_4N^+$	153.8	0.02
$(CH_3CH_2CH_2CH_2CH_2)_4N^+$	---	0.009

be obtained from figure 9-4 when the salt concentration is 3 mM. The area/molecule increases as the size of organic ions increases (Table 9-2).

9.3.1.4 Increased Intermolecular Distance Between Surfactant Molecules in the Adsorbed Film

The intermolecular distance of SDS at the interface can be calculated as follows. Let us assume that each SDS molecule at the interface occupies the square lattice with side 'a' as shown in figure 9-5. Thus, the area of a square lattice for a molecule is a^2, and the distance between two adjacent squares is 'a'. The area/molecule of SDS calculated as described in (9.3.1.3.) can be equated with a^2 and hence the intermolecular distance 'a' can be obtained by following equation;

$$(Intermolecular\ Distance) = a = (Area/Molecule)^{\frac{1}{2}} \qquad (9.5)$$

The intermolecular distance between SDS molecules at the air/water interface calculated by equation (9.5) increases with an increase in the size of organic ions (7.2 Å in aqueous solution, 10.5 Å in tetramethylammonium ion, 10.9 Å in tetraethylammonium ion, 11.5 Å in tetrapropylammonium ion and 12.4 Å in tetrabutylammonium ion solution when organic salt concentration is 3 mM) as shown in figure 9-6. This small increase in the intermolecular distance leads to a dramatic

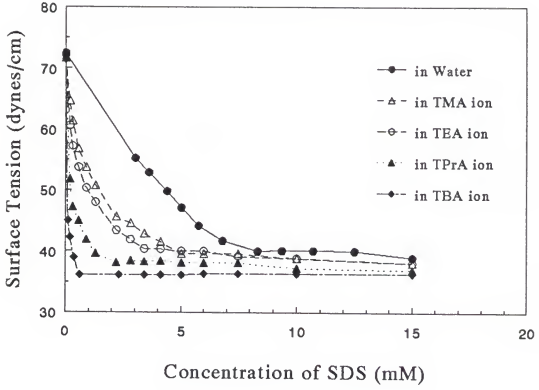

Figure 9-4 The surface tension of SDS solutions containing tetraalkylammonium ion. The concentration of organic salt was kept at 3 mM in all cases.

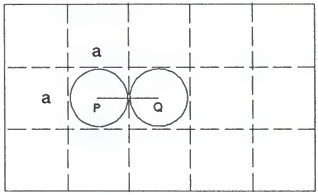

Figure 9-5 The square lattice model for the adsorbed monolayer of SDS at the interface used to calculate the intermolecular distance.

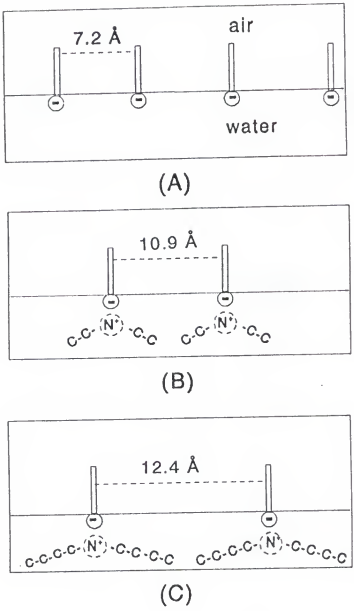

Figure 9-6 The average intermolecular distance for SDS films on water (A), 3 mM tetraethylammonium (B), and 3 mM tetrabutylammonium ionic solution (C).

decrease in surface viscosity of the SDS solution in the presence of organic ions (Table 9-2). It has been reported that the average area/molecule of stearic acid in the buffer solution was maximum at pH 9.0 because of the strongest repulsion between molecules, or the penetration of buffer ions.[142] The maximum area/molecule of the fatty acid at pH 9.0 resulted in the most unstable foam of decanoic acid. However, the addition of decanol to decanoic acid in the molar ratio of 3:1 strikingly improved the foam stability at pH 9.0.[143] The reduction in the interlayer electrical repulsions in presence of large tetraalkylammonium ions most certainly contributes to the destabilization of the foam. Since tetraalkylammonium ions are also found to substantially decrease the stability of nonionic foams (see section 9.3.2), the adsorption of these organic ions to surfactant films might be common to both ionic and nonionic surfactants. For SDS films, ionic interaction between surfactants and organic cations might enhance the adsorption of ions to the film. For nonionic films, the surface activity of organic cations could drive the cations to adsorb at the nonionic films.

9.3.1.5 Reduced CMC

Tetraalkylammonium ions are water structure formers and this effect increases with an increase in the length of the alkyl group.[17] Moreover, the degree of counterion association to the ionic surfactant layer increases with the size of ions. Therefore, the CMC of SDS in the 3 mM tetraalkylammonium solutions decreases

as the size of the organic ion increases. The CMC also decreases as the concentration of organic salts increases (Table 9-3 and Figures 9-7,8,9,10). The liquid film in foam must have a film elasticity such that mechanical shocks that tend to cause a local thinning or stretching of the liquid film are rapidly opposed and counterbalanced by the restoring forced generated during the initial stage of distortion. The mechanism concerning operation of this film elasticity depends on two phenomena: (1) the adsorption of surfactant monomers from the bulk to the air/water interface to restore the surface tension in expanding region (Gibbs effect) and (2) the movement of liquid to restore the thinning process by the gradient of surface tension (Marangoni effect).[17] When the CMC is low (i.e., the concentration of monomers is low), the surfactant monomers cannot adsorb quickly from the bulk to the air/water interface. This slow adsorption of monomer results in less film elasticity and less foam stability in the solution of SDS and tetraalkylammonium ions.

The Gibbs effect can be studied by using the surface elasticity defined as

$$E=2\left(\frac{d\gamma}{dA/A}\right) \tag{9.6}$$

The greater the value of E is, the greater the ability of film to resist the shocks on thinning. For a soluble surfactant system, elasticity of the film is found to be[17]

TABLE 9-3. The CMC of SDS solutions in various organic salt solutions of different concentrations. The CMC of SDS in pure aqueous solution is 8.2 mM.

Concentration of organic ion	3 mM	10 mM	50 mM
$(CH_3)_4N^+$	5.0 mM	2.3 mM	1.3 mM
$(CH_3CH_2)_4N^+$	3.4	2.2	0.9
$(CH_3CH_2CH_2)_4N^+$	1.6	1.0	0.36
$(CH_3CH_2CH_2CH_2)_4N^+$	0.62	0.31	0.12

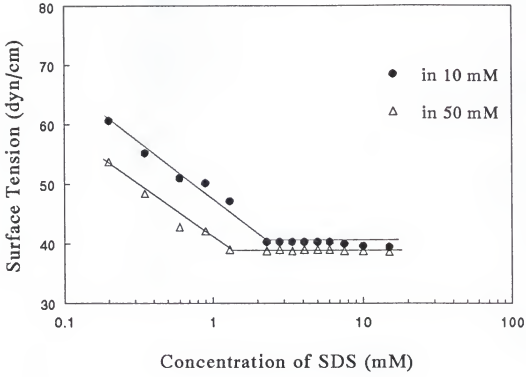

Figure 9-7 The surface tension of SDS solutions at 10 mM and 50 mM tetramethylammonium ionic concentration.

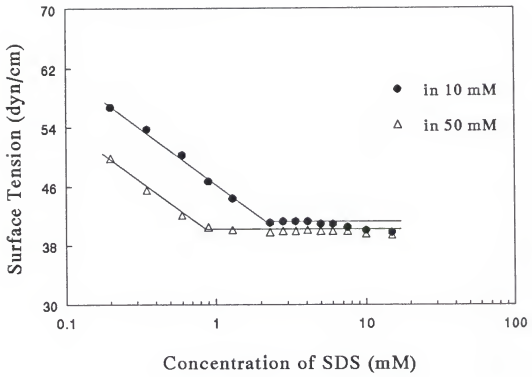

Figure 9-8 The surface tension of SDS solutions at 10 mM and 50 mM tetraethylammonium ionic concentration.

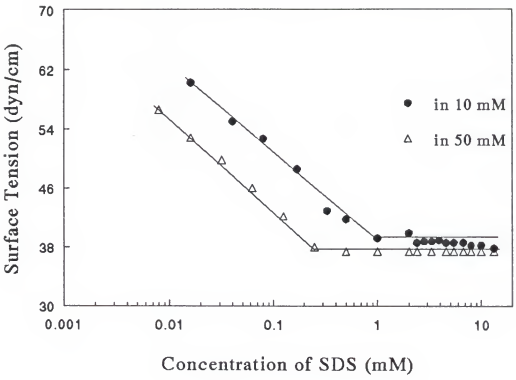

Figure 9-9 The surface tension of SDS solutions at 10 mM and 50 mM tetrapropylammonium ionic concentration.

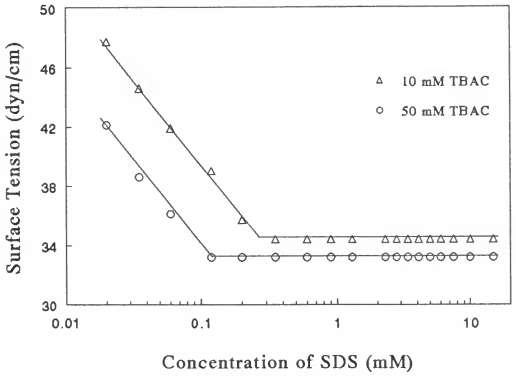

Figure 9-10 The surface tension of SDS solutions at 10 mM and 50 mM tetrabutylammonium ionic concentration.

$$E = \frac{4\Gamma^2 RT}{h_b C} \tag{9.7}$$

where Γ is the surface excess concentration, C is the concentration of surfactant in the bulk and h_b is the film thickness. It shows that there is no film elasticity when Γ is zero. This is the reason why the pure solution can not make foam. Also surface elasticity decreases with the thickness of film and the concentration of surfactant in the bulk.

9.3.2 Comparison with Other Antifoaming Substances

A comparison of the foam destabilizing efficiency of electrolytes with the largest tetraalkylammonium ions, TBAB and TPAB, with some other well-known antifoaming substances, tributyl phosphate (TBP) and 2-ethyl hexanol (EH) was made. Figure 9-11 shows the half-life of foams stabilized by SDS in the presence of different foam inhibiting substances. TPAB was found to be more effective in destabilizing the foam than TBP, whereas the efficiency of TBAB was slightly lower. The $\tau_{1/2}$ values obtained for the foams in the presence of TBP and the organic salts are rather similar, however. Since tributyl phosphate acts by promoting drainage of the lamella by reducing the surface viscosity of the surfactant films,[129] this indicates that a similar mechanism may be attributed to the tetraalkylammonium ions. The

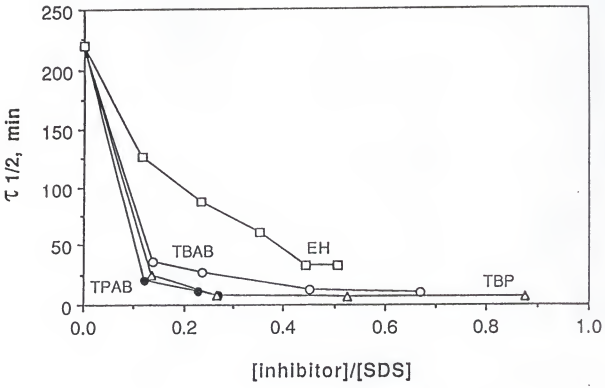

Figure 9-11 The half-life, $\tau_{1/2}$, of SDS foams in the presence of different foam inhibitors versus the inhibitor/surfactant molar ration. The SDS concentration was 14 mM. In absence of electrolyte, $\tau_{1/2}$ was 225 minutes.

surface tension of TBP is 27 mN/m, whereas the surface tension of a 1 M solution of TBAB is 46 mN/m. As may be seen from figure 9-12, which shows the half-lifes of foams produced with hexaethylene dodecyl ether, $C_{12}E_6$, TBP is much more effective in destabilizing the nonionic surfactant system than TPAB. This may be attributed to a lower surface concentration of TPAB compared to TBP in this system which does not include the coulombic attraction between SDS and TPAB as was in the previous system.

In both the anionic and nonionic surfactant systems, 2-ethyl hexanol is less efficient in destabilizing foams, compared to the organic salts. Although the surface activity is higher for EH (the surface tension is 26 mN/m), it may not expand the area/molecule as efficiently as tetraalkylammonium ions due to the molecular shape. Therefore, it is not very effective as the antifoaming agent.

In many practical applications, foams are stabilized by mixtures of ionic and nonionic surfactants. The influence of TPAB and TBP on the foam stability of mixed SDS and $C_{12}E_6$ surfactant systems were therefore studied. The ratio between SDS and $C_{12}E_6$ was altered, whereas both the total surfactant concentration and the concentration of foam inhibitors were kept constant. In agreement with what was observed above, TPAB was found to be more efficient in destabilizing the foam in a pure ionic system compared to TBP, whereas the opposite was true in the pure

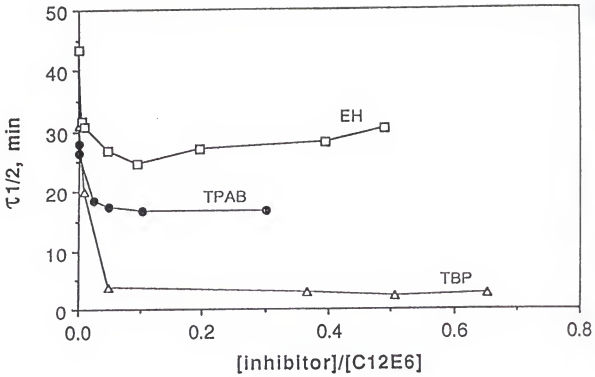

Figure 9-12 The half-life, $\tau_{1/2}$, of $C_{12}E_6$ foams in the presence of different foam inhibitors versus the inhibitor/surfactant molar ratio. The $C_{12}E_6$ concentration was 0.14 mM.

nonionic system, as may be seen from figure 9-13. In a mixed surfactant system no distinct differences between the two systems were observed. Hence, it appears that even at moderate surface potentials TPAB is as efficient as TBP in destabilizing these foams.

The comparison of the foam destabilizing efficiency of the tetraalkylammonium bromide salts with tributyl phosphate and 2-ethyl hexanol, which are used in many commercial foam inhibiting formulations, demonstrates that the organic salts have a potential for being useful in technical applications involving foam inhibition. By contrast to most defoamers/antifoamers used commercially, the tetraalkylammonium salts are water soluble. From a technical point of view this may be relevant, since it will facilitate the distribution of the foam inhibitor into the solutions which should be protected from foaming.

9.4 Conclusions

The addition of electrolyte containing tetraalkylammonium ions to foams stabilized by both ionic and nonionic surfactants leads to

1) an increase in the area/molecule of surfactant at the air/water interface,

2) a decrease in the surface viscosity due to the increased area/molecule,

3) a decrease in the CMC of surfactant, and hence the decrease in concentration of

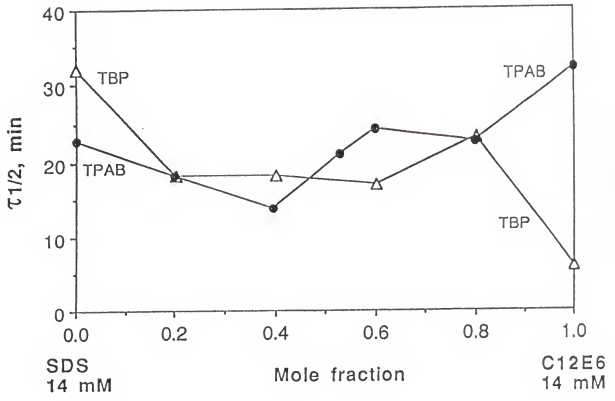

Figure 9-13 The half-life, $\tau_{1/2}$, of foams stabilized by mixtures of $C_{12}E_6$ and SDS in the presence of different foam inhibitors. The ratio between SDS and $C_{12}E_6$ was altered, whereas the total surfactant concentration, 14 mM and the concentration of foam inhibitors, 3 mM were kept constant.

surfactant monomers in the solution.

4) a decrease in foam stability due to the above-mentioned factors.

The destabilizing efficiency of the organic salts is related to the size of the tetraalkylammonium ions. The larger the size of tetraalkylammonium ion, the more effective it is as a foam destabilizing agent.

A comparison between the foam destabilizing efficiency of tetraalkylammonium ions with tributyl phosphate and 2-ethyl hexanol demonstrated that organic ions have a potential for being useful in technical applications involving foam inhibition.

CHAPTER 10
ESTERIFICATION OF STEARIC ACID WITH GLYCEROL BY LIPASE IN FOAM

10.1 Introduction

The enzymic synthesis of mono-, di- and triglycerides has been studied extensively to understand the mechanism of reaction between oil-soluble fatty acid and water soluble glycerol by the enzyme (Lipase) in reverse micellar solutions.[144-145] The anionic double-tailed surfactant AOT [sodium di-(2-ethylhexyl) sulfosuccinate] is most frequently used to form reverse micelles. Unlike most surfactants, AOT does not require additional amphiphiles as cosurfactants for the formation of reverse micelles because of its wedge-shaped molecular geometry.[146] The rate of enzymic reaction in reverse micelles depends on the surfactant concentration, the water to surfactant ratio, the temperature and concentration of buffers as well as co-and counterions present.[147] Previous studies[148-149] showed that the ratio of mono-, di- and triglycerides formed in the reverse micelles is influenced by the pH, temperature and reaction time. The reaction at the oil/water interface in reverse micelles yields predominantly diglyceride and a very small amount of mono- and triglycerides. It has

been reported that the products in reverse micelles contain 50 % diglyceride, 10 % monoglyceride and less than 3 % of triglyceride.[150]

However, commercial scale-up of such an enzymic synthetic process has not been reported presumably due to various limitations as the products are intended for use as food, cosmetic or pharmaceutical ingredients. Recently several studies have been reported on the enzymic synthesis in solvent-free systems in an attempt to make the process commercially feasible. These efforts not only excluded the toxicity problem of the solvents and surfactants, but also reduced many steps in the purification process. Kim et al.[151] have reported the enzymic synthesis in dispersions of capric acid and water in a surfactant-free system. The mixture of capric acid and glycerol was agitated vigorously by a magnetic stirrer in an open glass vial, and the reaction was initiated by adding the lipase into the reaction mixture. The products in this system were very similar as compared to that in the reverse micellar solution when the molar ratio of capric acid to glycerol is greater than 3.0; namely, a large amount of diglyceride and small amounts of mono- and triglyceride were obtained by the enzymic reaction.

The present study reports the enzymic synthesis in foam as a solvent and surfactant-free system. Foam can provide a large interfacial area at which the synthetic reaction can occur. In this study, stearic acid was used as the foaming agent as well as one of the reactants.

10.2 Experimental Procedure

15 ml of double distilled-water and 15 ml of glycerol (Fisher Scientific Co.) were added into a glass column (4 cm of diameter x 100 cm length). A 0.2 g of stearic acid was dissolved in 4 ml of chloroform, then added into the column. Without this process the stearic acid molecules did not dissolve in the solution. Air was blown at a high flow-rate for 15 minutes to evaporate all chloroform before adding the enzyme because the organic solvent inhibits the activity of the enzyme. A 0.2 ml of Lipozyme 10000 L supplied by the Novo company was added into the column. The enzyme catalyzes the esterification of glyceride as well as enhance the foaming of solution. Air was continuously blown during the reaction to maintain a large foam volume (Figure 10-1). The samples were taken after a reaction time of 15 min., 30 min., 1 hr and 2 hr. A 1.5 ml of iso-octane and 2-propanol mixture (4:1 v/v) was added to each sample immediately after removal from the foam column to stop the enzymic reaction.

Normal phase HPLC with UV absorbance detector of 213 nm cut-off wavelength and 0.05 auf was used to analyze the product of reaction at various time intervals. The silica column (10 cm x 2.4 cm) and the mixture of iso-octane and 2-propanol (96:6 v/v) as a mobile phase were used at room temperature. The flow-rate of mobile phase was kept at 1 ml/min. The absorbance detector of the HPLC is from Spectra Physics (Model SP8450). The integrator (Model SP8880) plots raw

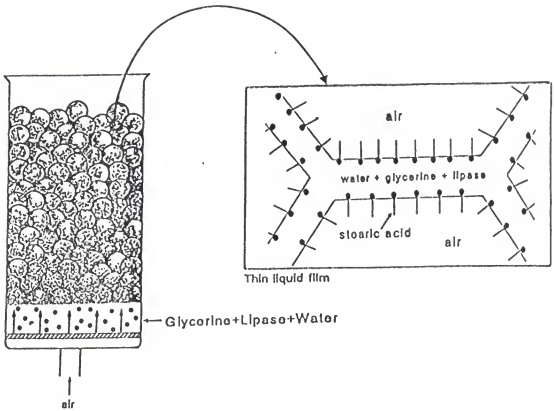

Figure 10-1 A schematic diagram of the foam column and expanded representation of a thin film in foam.

signals from the detector and determines the presence of peaks. This signal is analyzed by Spectra Physics software, LNET2 and SPMENU.

10.3 Results and Discussion

The results are shown in figure 10-2. In contrast to the products formed in the reverse micelles,[152] the reaction in foam produced a large amount of triglyceride (almost 20 %) as well as a large amount of diglyceride (55 %). The difference in the quantity of di- and triglyceride produced in the foam versus reverse micelles can be explained on the basis of the two-phase model proposed by Verger[153] for phospholipase catalyzed hydrolysis of phospholipid monolayers because the reaction in foam also takes place at the air/water interface. In this model, the entrance of the water-soluble enzyme into the monolayer is the first step. The second step is the formation of the enzyme-substrate complex within the monolayer. In the catalytic step the product is formed and the enzyme is regenerated. If the product is water-soluble, it will migrate into the aqueous phase. If the product is oil-soluble, the product will remain at the air/water interface, resulting in other consecutive reactions.

Figure 10-3 shows an expanded diagram of the thin liquid film in the foam before and after the esterification reaction. The molecules of stearic acid at the interface react with glycerol in water phase by the Lipozyme. In a very short time

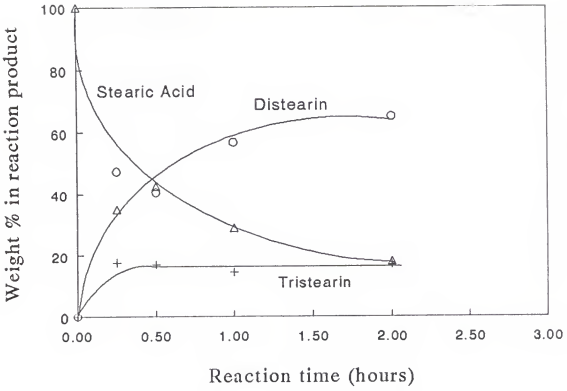

Figure 10-2 Weight % of each component in the reaction product vs. reaction time.

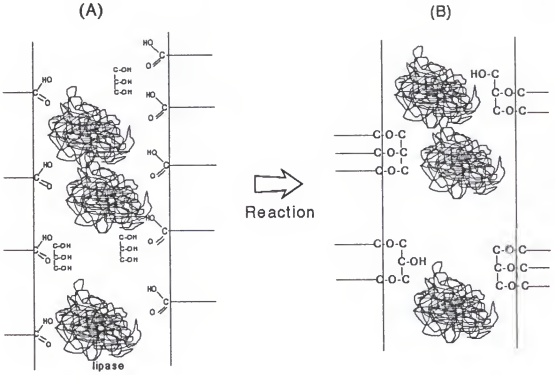

Figure 10-3 Reaction mechanism for esterification in liquid thin film, (A) before reaction and (B) after reaction.

period (~5 min.), most of the reaction products might be diglyceride because the enzyme has specific activity for 1,3-diglyceride, but the specificity is not so strict in this esterification reaction.[154] Also the amount of diglyceride increases as the reaction time increases before the reaction reaches the equilibrium state as shown in figure 10-2. With further increase in reaction time, diglyceride produced may get converted into the triglyceride because diglyceride would stay at the air/water interface in foam. In contrast, the diglyceride formed at the oil/water interface in reverse micellar solution may partition into the oil phase. Therefore, the main product in the reverse micelles is diglyceride.

The reaction was also carried out in foam but without the addition of lipase. There was no significant change in the concentration of stearic acid after 3 hours. Thus, the presence of lipase is required in foam to produce di- and triglycerides.

In summary, the esterification reactions by enzyme in foam which involves the air/water interface yielded products in different proportions as compared to that produced by the reverse micellar solutions and other solvent-free systems (e.g., dispersions). The reaction in foam produced large amounts of diglyceride (~55 wt%) as well as triglyceride (~20 wt%), whereas the reaction in the reverse micelles produced large amounts of diglyceride only (~50 wt %), less monoglyceride (~ 10 wt %) and a much less amount of triglyceride (less than 3 %). The absence of monoglyceride in foam is probably due to the preferred orientation of stearic acid

and the absence of surfactant at the air/water interface which favors further esterification resulting in diglyceride. It should be emphasized that the percent conversion of fatty acid into glyceride in the reverse micellar system is about 70 %, whereas in foam it is about 80 %. The reaction in foam can be employed for large scale production of di- and triglycerides using enzymes due to a large air/water interface at which the reaction takes place without using solvents or surfactants.

CHAPTER 11
CONCLUSIONS AND RECOMMENDATIONS FOR FUTURE WORK

11.1 Relaxation Time (τ_2) of SDS Micelles

Relaxation time (τ_2) of SDS micelles, which is related to micellar lifetime, was measured by pressure-jump method. The relaxation times of micelles were in the range of 1 millisecond to 10 seconds depending upon the concentration. This change was more than four orders of magnitude. The relaxation time of SDS micelles was maximum at 200 mM surfactant concentration due to the strongest electric repulsion between micelles, which hampered the dissociation of micelles.

11.2 Foamability in Micellar Solutions

During foam generation, surfactant monomers adsorb from the bulk to the air/water interface to stabilize the liquid thin film. Foam can not be generated without this process. Additional surfactant monomers should be supplied by the dissociation of micelles after all initial surfactant monomers adsorb into the air/water interface. Since stable micelles can not breakdown quickly during the foaming process, enough surfactant monomers can not be supplied to the air/water interface.

As a result of this phenomena, greater micellar stability leads to decreased foaming ability of micellar solutions.

11.3 Bubble Dynamics

The bubble detaches itself from the capillary tip if its buoyancy force exceeds the surface tension force at the tip/bubble interface when the bubbles are generated in solution by air-flowing through the capillary. Surfactant monomers adsorb from the bulk to the air/water interface during the bubble growth. If surfactant monomers can not adsorb into the interface quickly, the dynamic surface tension is high. This high dynamic surface tension results in large bubble size. Surfactant monomers can not adsorb quickly to the interface if micelles are stable due to slow breakdown of micelles. Therefore, the bubble size increases as the stability of micelles increases.

11.4 Textile Wetting

Textile wetting involves lots of replacement of air with solution in capillaries of a fabric. The rate of replacement depends on the dynamic surface tension at the air/solution interface of the wetting front. Also the micellar stability influences the dynamic surface tension of micellar solutions by the same reason explained in the previous section. The wetting time was maximum at 200 mM SDS concentration, at which the most stable micelles are formed.

11.5 Emulsion Droplet Size

The emulsion droplet size was also maximum at 200 mM SDS concentration in the mixture of hexadecane/surfactant solution mixtures. The droplet size of an emulsion is determined by equation (5.1). When same amount of energy is applied to the oil/water mixture, the decrease in dynamic surface tension results in a smaller droplet size (i.e., a larger change in interfacial area). If micelles are stable, the flux of surfactant monomers from the bulk to the oil/water interface is small, which leads to high dynamic surface tension. Thus, emulsion droplet size is large due to high dynamic surface tension.

11.6 Solubilization

The rate of solubilization of benzene and Orange OT dye into SDS solutions was maximum at 200 mM SDS concentration due to the hydrophobicity of the cores of micelles. The intermicellar distance decreases as the surfactant concentration (or the number of micelles) increases, resulting in the stronger electric repulsion between micelles. Therefore, micelles become more rigid due to the compressive force of intermicellar repulsion as the concentration increases up to 200 mM of SDS. With further increase in SDS concentration, the shape of micelles changes from spherical to cylindrical shape to accommodate more surfactant molecules in the solution and to minimize the free energy of the system. The interior of the tightly packed micelles

is more hydrophobic than that of loosely packed micelles and therefore the tightly packed micelles induce rapid solubilization of non-polar molecules (e.g., benzene, Orange OT, etc.) into these micelles.

In summary, foaming ability, bubble dynamics, textile wetting, emulsion droplet size and rate of solubilization are all related to the micellar stability and hence to the micellar lifetime. All these results are summarized in figure 11-1.

11.7 Recommendations for Future Work

Our understanding of the effect of micellar lifetime on the various technological processes such as foaming, bubble dynamics, wetting, emulsification and solubilization is still far from completion. There is a great need for further study. The work presented in this dissertation has answered the following questions:

1) Why does micellar structure change from spherical to cylindrical shape as the surfactant concentration increases?

2) Why is micellar stability maximum at 200 mM SDS concentration?

3) How does the hydrophobicity of the micellar core change with SDS concentration, and how does hydrophobicity influence the rate of solubilization?

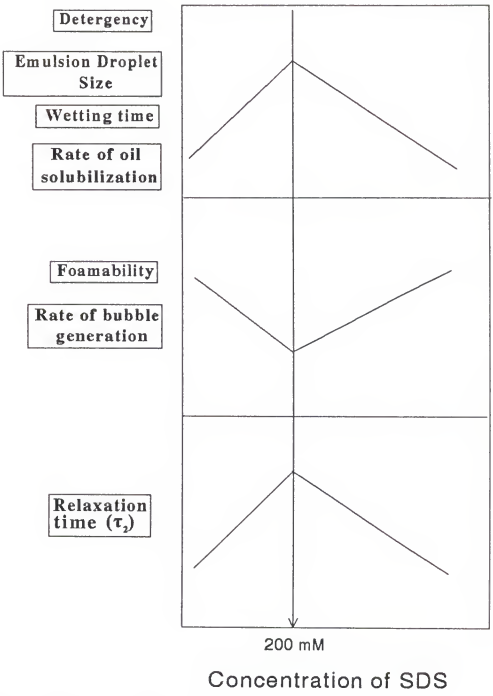

Figure 11-1 Summary of all experimental results.

4) How does micellar stability play an important role in dynamic technological processes?, etc.

Many additional questions were raised through this study. The following sections contain recommendations for future research into these subjects. The general areas are i) direct measurement of dynamic surface tension, ii) salt effect on micellar kinetics, iii) theoretical modelling, and iv) other surfactant systems except SDS.

11.7.1 Direct Measurement of Dynamic Surface Tension

In this study, all results were explained on the basis of micellar life-time, which influences the rate of surfactant monomer adsorption to the interface. This rate determines the dynamic surface tension of micellar solutions. The dynamic surface tension of SDS micellar solutions as a function of concentration was not measured in this study.

11.7.2 Salt Effect

The life-time of micelles can be changed significantly by the addition of salt (NaCl, LiCl, CsCl, etc.) into the micellar solution. Also the maximum point in the curve of micellar relaxation time vs. concentration will shift in salt solution. It is highly recommended to study this effect due to its practical importance, because all industrial applications of surfactants involve the presence of salt.

11.7.3 Theoretical Modeling

The explicit finite difference method was used to solve the diffusion equations for micelles and surfactant monomers in the solution, and Henry's adsorption isotherm was used for the surfactant monomer adsorption at the surface. It is recommended to use implicit finite difference method or finite element method for the diffusion equation, and the Langmuir adsorption isotherm, Volmer isotherm or Freundlich adsorption isotherm for adsorption phenomena at the surface to get more accurate mathematical values.

11.7.4 Other Surfactant Systems

In this study, SDS was chosen as the surfactant to investigate the effect of micellar lifetime on various technological processes. It is recommended that similar experiments should be done on other surfactant systems to generalize all of the explanations given in this thesis.

APPENDIX A
COMPUTER PROGRAM

```
C
C-------------------------------------------------
C     SOLUTION FOR SURFACTANT MONOMER ADSORPTION
C     INTO SURFACE FROM BULK IN MICELLAR SOLUTION
C     BY FINITE DIFFERENCE METHOD
C-------------------------------------------------
C
C
      DIMENSION A(501,501),B(501,501)
      OPEN(UNIT=55,FILE='TAPE55',STATUS='OLD')
C
C-------------------------------------------------
C     INITIAL CONDITIONS
C-------------------------------------------------
C
      A(1,1)=0.0
      B(1,1)=0.0
C
C-------------------------------------------------
C     BOUNDARY CONDITIONS
C-------------------------------------------------
C
      DO 10 K=2,500,1
      A(500,K)=1.0
      B(500,K)=1.0
      A(K,1)=1.0
      B(K,1)=1.0
      B(1,K)=0.0
      B(2,K)=0.0
   10 CONTINUE
C
C-------------------------------------------------
C     STEP SIZE
C-------------------------------------------------
C
      XK=0.01
      XH=0.2
C
```

```
C-------------------------------------------------------------
C     VALUES OF PARAMETERS
C-------------------------------------------------------------
C
      N=100
      ALPH1=0.0001
      ALPH2=0.313
      ALPH3=0.038
C
       XX=XK/(XH**2)
       X1=ALPH3*XK
       X2=(ALPH3*XK)/(N*ALPH2)
       X3=XK/(2*XH)
C
C
       DO 50 J=1,500,1
       DO 30 I=2,500,1
C
C-------------------------------------------------------------
C     GOVERNING EQUATION FOR SURFACTANT MONOMERS
C-------------------------------------------------------------
C
      A(I,J+1)=XX*(A(I+1,J)-2*A(I,J)+A(I-1,J))+A(I,J)
     &-(X1)*(A(I,J)**N-B(I,J))
C
C-------------------------------------------------------------
C     GOVERNING EQUATION FOR MICELLES
C-------------------------------------------------------------
C
      B(I,J+1)=B(I,J)+X2*(A(I,J)**N-B(I,J))+(XX*ALPH1)
     &*(B(I+1,J)-2.0*B(I,J)+B(I-1,J))
C
C-------------------------------------------------------------
C     ADSORPTION ISOTHERM
C-------------------------------------------------------------
C
      A(1,J+1)=A(1,J)+(XK/XH)*(A(2,J)-A(1,J))
C
   30 CONTINUE
   50 CONTINUE
C
       WRITE (55,'(8F8.4)') (A(1,J), J=1,500)
C      WRITE(6,'(8F8.4)') (A(1,J) ,J=1,500)
       CLOSE (55)
       END
```

REFERENCES

1. J.H. Fendler, "Membrane Mimetic Chemistry," John Wiley & Sons, Inc., New York (1982), chapter 2.

2. C. Tanford, "The Hydrophobic Effect," John Wiley & Sons, Inc., New York (1973).

3. P.A. Winsor, Chem. Rev., 68, 1 (1968).

4. R.D. Vold and M.J. Vold, "Colloid and Interface Chemistry," Addison-Wesley Inc., London (1983).

5. A.D. James, B.H. Robinson and N.C. White, J. Colloid Interface Sci., 59, 328 (1977).

6. C. Tondre, J. Lang and R. Zana, J. Colloid Interface Sci., 52, 372 (1975).

7. H. Hoffman, R. Nagel, G. Platz and W. Ulbricht, Colloid & Polymer Sci., 254, 812 (1976).

8. D.A.W. Adair, V.C. Reinsborough, N. Plavac and J.P. Valleau, Can. J. Chem., 52, 429 (1974).

9. D.A.W. Adair, V.C. Reinsborough, H.M. Trenholm and J.P. Valleau, Can. J. Chem., 54, 1162 (1976).

10. E.A.G. Aniansson and S.N. Wall, J. Phys. Chem., 78, 1024 (1974).

11. H.L. Rosano and M. Clausse, "Microemulsion System," Marcel Dekker Inc., New York (1987).

12. D. Attwood, A.T. Florence, "Surfactant Systems," Chapman and Hall Ltd., London (1983), chapter 3.

13. R. Leung, D.O. Shah, J. Colloid Interface Sci., 113, 484 (1986).

14. N. Muller, "Solution Chemistry of Surfactant," K.L. Mittal (Ed.), Plenum Press, vol. 1, pp267-295, New York (1979).

15. B. Chance, "Techniques of Organic Chemistry," 3 rd ed., vol. 4, part 2, G.G. Hammond (Ed.), Wiley, New York (1974), chapter 2.

16. H.H. Gruenhagen, J. Colloid Interface Sci., 53, 282 (1975).

17. M.J. Rosen, "Surfactants and Interfacial Phenomena," John Wiley & Sons, Inc. (2nd ed.), New York (1989).

18. M.J. Jaycock and R.H. Ottewill, " Proc. 4th International Congr. Surface Active Substance," vol. 2, p. 545, Gordon and Breach Science Publisher, New York (1967).

19. E.A.G. Aniansson, S.N. Wall, M. Almgren, H. Hoffmann, Kielmann, W. Ulbricht, R. Zana, J. Lang and C. Tondre, J. Phys. Chem., 80, 905 (1976).

20. D. Hull, P.L. Waynes, and J.E. Rassing, J. Chem. Soc. Faraday Trans. 2, 73, 1582 (1977).

21. J. Lang, "Surfactants in Solution," K.L. Mittal and P. Bothorel (Eds.), vol. 4, p. 299, Plenum Press, New York (1984).

22. M. Tanaka, S. Kaneshina, S. Kuramoto and R. Matuura, Bull. Chem. Soc. Japan, 48, 432 (1975).

23. E. Lessner, M. Teubner, and M. Kahlweit, J. Phys. Chem., 85, 3167 (1981).

24. E. Lessner and J. Frahm, J. Phys. Chem., 86, 3032 (1982).

25. M. Kahlweit, J. Colloid Interface Sci., 90, 92 (1982).

26. P. Lianos and R. Zana, J. Colloid Interface Sci., 84, 100 (1981).

27. J.B. Hayter and J. Penfold, J. Chem. Soc., Faraday Trans. I, 77, 1851 (1981).

28. P. Ekwall, "Some Properties of Association Colloid Solutions above CMC: Chemistry, Physics and Application of Surface Active Substance," J.Th.G. Overbeek (Ed.), Gordon and Breach Science Publisher, New York (1967).

29. W.J. Gettings, J.E. Rassing, E. Wyn-Jones, "Micellization, Solubilization and Microemulsion," K.L. Mittal (Ed.), Plenum Press, vol. 1, p. 347, New York (1977).

30. M.V.D. Auweraer, E. Roelants, A. Verbeeck and F.C.De. Schryver, "Surfactants in Solution," K.L. Mittal (Ed.), Plenum Press, vol. 7, p. 141, New York (1989).

31. D.H. Everett, "Basic Principles of Colloid Science," Royal Society of Chemistry, London (1988).

32. F.Q. Tang, Z. Xiao, Ji-An Tang and L. Jiang, J. Colloid Interface Sci., 131, 498 (1989).

33. S.E. Friberg, I. Blute and H. Kunieda, Langmuir, 2, 659 (1986).

34. F.D. Smith, A.J. Stirton and M.V. Nunez-Ponzoa, J. Am. Oil Chem. Soc., 43, 501 (1966).

35. J.J. Bikeman, "Foams," Springer-Verlag New York Inc., pp237-238, New York (1973).

36. S. Ross, " Encyclopedia of Chemical Tcchnology," John Wiley & Sons Inc. (3rd ed.), vol. 11, pp127-145, New York (1980).

37. S.E. Friberg, I. Blute and P. Stenius, J. Colloid Interface Sci., 127, 573 (1989).

38. D.O. Shah, J. Colloid Interface Sci., 37, 744 (1971).

39. T. Szekrenyesy, K. Liktor and N. Sandor, Colloids and Surfaces, 68, 267 (1992).

40. R. Buscall and R.H. Ottewill, "Colloid Science," D.H. Everett (Ed.), The Chemical Society, vol.2, London (1975).

41. C.A. Miller and P. Neogi, "Interfacial Phenomena: Equilibrium and Dynamic Effects," Marcel Dekker Inc., New York and Basel (1985), chapter 5.

42. D.O. Shah, N.F. Djabbarab and D.T. Wasan, Colloid & Polymer Sci., 256, 1002 (1978).

43. H. Schott, J. Am. Oil Chem. Soc., 65, 1658 (1988).

44. D.O. Shah, M.K. Sharma and W.E. Brigham, SPE Reservoir Engineering, May, 253 (1986).

45. D.S.H. Sarma, J. Pandit and K.C. Khilar, J. Colloid Interface Sci., 124, 339 (1988).

46. A.D. Ronteltap, B.R. Damste, M.De Gee and A. Prins, Colloids Surface, 47,

269 (1990).

47. A. Prins, "Advances in Food Emulsions and Foams," E. Dickinson and G. Stainsby (Eds.), Elsevier Applied Science, London (1988), chapter 3.

48. T.F. Ling, "Surface properties and Flow Behavior of Foam in Relation to Fluid Displacement in Porous Media," Ph.D. Dissertation, University of Florida, Gainesville, (1987).

49. J.T. Davies and E.K. Rideal, "Interfacial Phenomena," Academic Press (2nd ed.), p. 408, New York (1963).

50. D.T. Wasan and A.D. Nikolov, J. Colloid Interface Sci., 133, 1 (1989).

51. D.T. Wasan, I.B. Ivanov, A.D. Nikolov and P.A. Kralchevsky, Langmuir, 6, 1180 (1990).

52. M.J. Rosen and Z.H. Zhu, J. Am. Oil Chem. Soc., 65, 663 (1988).

53. M.K. Sharma, D.O. Shah and W.E. Brigham, J. AICHE, 31, 222 (1985).

54. S. Ross and G. Nishioka, J. Phys. Chem., 79, 1561 (1975).

55. J.Th.G. Overbeek, J. Colloid Interface Sci., 58, 408 (1977).

56. T. Inoue, Y. Shibuya and R. Shimozawa, J. Colloid Interface Sci., 65, 370 (1978).

57. M.K. Sharma, D.O. Shah and W.E. Brigham, I&EC Fundamentals, 23, 213 (1984).

58. J.K. Borchardt and C.W. Yates, J. Am. Oil Chem. Soc., 70, 47 (1993).

59. C. Jho, and R. Burke, J. Colloid Interface Sci., 95, 61 (1983).

60. R. Miller, R. Sedev, K.H. Schano, C. Ng and A.W. Neumann, Colloids and Surfaces, 69, 209 (1993).

61. W.D.E. Thomas and D.J. Hall, J. Colloid Interface Sci., 51, 328 (1975).

62. L. Kelvin, Phil. Mag., 42, 368 (1871).

63. C.A. MacLeod and C.J. Radke, J. Colloid Interface Sci., 160, 435 (1993).

64. K.J. Mysels, Langmuir, 2, 428 (1986).

65. J.L. Ross, W.D. Bruce and W.S. Janna, Langmuir, 8, 2644 (1992).

66. M.J. Rosen, and X. Y. Hua, J. Colloid Interface Sci., 124, 652 (1988).

67. D.R. Ward and P.R. Garrett, J. Colloid Interface Sci., 132, 475 (1989).

68. R. Clift, J. R. Grace and M. E. Weber, "Bubbles, Drops and Particles," Academic Press, New York (1978).

69. R.E. Joos, J. Phys. Chem., 86, 3471 (1982).

70. J.V. Hunsel and P. Joos, Colloid & Polymer Sci., 267, 1026 (1989).

71. S.G. Oh and D.O. Shah, Langmuir, 7, 1316 (1991).

72. B. Fainerman and A.V. Makievski, Colloids and Surfaces, 69, 249 (1993).

73. B. Fainerman, Colloids and Surfaces, 62, 333 (1992).

74. M. Austin, B.B. Bright and E.A. Simpson, J. Colloid Interface Sci., 23, 108 (1967).

75. M. Dahanayake, A. W. Cohen and M. J. Rosen, J. Phys. Chem., 90, 2413 (1986).

76. F.M. Fowkes, J. Phys. Chem., 57, 98 (1953).

77. A. Gerault, Fed. Assoc. Techniciens Ind. Peintures, Vernis, Emaux Encres Imprimerie Europe Continentale Congr., 7, 119 (1964).

78. M. Dahanayake, Ph.D. Dissertation, City University of New York, New York, (1985).

79. W. Griess, Fette, Seifen, Anstrichem., 57, 24 (1955).

80. M.J. Schwuger, J. Am. Oil Chem. Soc., 59, 258 (1982).

81. J.K. Weil, A.J. Stirton and R.G. Bistline, J. Am. Oil Chem. Soc., 31, 444 (1954).

82. A.K. Biswas and B.K. Mukherji, J. Appl. Chem., 10, 73 (1960).

83. E.W. Washburn, Phys. Rev. Ser., 17, 273 (1921).

84. E.K. Rideal, Phil. Mag., 44, 1152 (1922).

85. A.W. Adamson, "Physical Chemistry of Surfaces," John Wiley & Sons Inc. (4th ed.), New York (1982), chapter 13.

86. P.H. Elworthy and K.J. Mysels, J. Colloid Sci., 21, 331 (1966).

87. F.E. Bartell and L.S. Bartell, J. Am. Chem. Soc., 56, 2205 (1934).

88. K. Shinoda, S.E. Friberg, "Emulsions and Solubilization," John Wiley & Sons Inc., New York (1986).

89. B.J. Caroll, "Surface and Colloid Science," E. Matijevic (Ed.), John Wiley & Sons Inc., New York (1976).

90. M.E. Karaman, L. Meagher and R.M. Pashley, Langmuir, 9, 1220 (1993).

91. P. Walstra, "Encyclopedia of Emulsion Technology," P. Becher (Ed.), vol.1, Marcel Dekker Inc., New York and Basel (1983).

92. V.G. Levich, "Physicochemical Hydrodynamics," Prentice-Hall Inc., Englewood Cliffs, NJ (1962).

93. P.J. Missel, N.A. Mazer, G.B. Benedek and M.C. Carey, J. Phys. Chem., 87, 1264 (1983).

94. P. Mukerjee, Adv. Colloid & Interface Sci., 1, 241 (1967).

95. P. Missel, N.A. Mazer, M.C. Carey and G.B. Benedek, J. Phys. Chem., 93, 8354 (1989).

96. G.J. Buist, C.A. Bunton, L. Robinson, L. Sepulveda and M. Stam, J. Am. Oil Chem. Soc., 93, 3002 (1971).

97. J.N. Israelachvili, "Intermolecular and Surface Force," Academic Press Inc., New York (1992), chapter 4.

98. E.L. Cussler, " Diffusion: Mass Transfer in Fluid Systems," Cambridge University Press, Cambridge (1984), chapter 6.

99. P.C. Hiemenz, "Principles of Colloid and Surface Chemistry," Marcel Dekker Inc., New York (1977).

100. D. Langevin, "Microemulsions: Structure and Dynamics," S.E. Friberg and P.

Bothorel (Eds.), CRC Press, Boca Raton, FL (1986), chapter 7.

101. S.E. Friberg and G. Rong, Langmuir, 4, 796 (1988).

102. J.H. Fendler and E.J. Fendler, "Catalysis in Micellar and Macromolecular Systems," Academic Press Inc., New York (1975), chapter 3.

103. A.T. Florence, I.G. Tucker and K.A. Walters, "Structure/Performance Relationships in Surfactants," M.J. Rosen (Ed.), ACS Symp. Series 253, American Chemical Society, p. 189, Washington DC (1984).

104. W. Philippoff, J. Colloid Interface Sci., 5, 169 (1950).

105. P. Mukerjee and J.R. Cardinal, J. Phys. Chem., 82, 1620 (1978).

106. J.C. Eriksson and G. Gillberg, Acta. Chem. Scand., 20. 2019 (1966).

107. S. Karaborni, N.M. van Os, K. Esselink and P.A.J. Hilbers, Langmuir, 9, 1175 (1993).

108. F. Tokiwa, J. Phys. Chem., 72, 1214 (1968).

109. J.H. Collett, R. Withington and L. Koo, J. Pharm. Pharmac., 27, 46 (1975).

110. H.B. Klevens, Chem. Rev., 47, 1 (1950).

111. T.R. Bates, M. Gibaldi and J.L. Kanig, J. Pharm. Sci., 55, 191 (1966).

112. R.S. Stearns, H. Oppenheimer, E. Simon and W.D. Harkins, J. Chem. Phys., 15, 496 (1947).

113. T. Nakagawa and K. Tori, Kolloid-Z.u.Z-Polymere, 194, 143 (1964).

114. T. Nakagawa and H. Jizomoto, Kolloid-Z.u.Z-Polymere, 250, 594 (1972).

115. A.F. Chan, D.F. Evance and E.L. Cussler, J. AICHE, 22, 1006 (1976).

116. K.S. Chan, "The molecular mechanism of achieving ultra-low interfacial tension in surfactant-oil-brine system," University of Florida, Gainesville (1978).

117. R. Miller, A. Hofmann, R. Hartmann, K-H Schano and A. Halbig, Advanced Materials, 4, 370 (1992).

118. R. Miller, G. Loglio and U. Tesei, Colloid & Polymer Sci., 270, 598 (1992).

119. S.R. Milner, Phil. Mag., 13, 96 (1907).

120. A.F.H. Ward and L. Tordai, J. Chem. Phys., 14, 453 (1946).

121. R. Miller and G. Kretzschmar, Adv. in Colloid & Interface Sci., 37, 97 (1991).

122. R. Wustneck, R. Miller and G. Czichocki, Tenside Surfactants Detergents, 29, 265 (1992).

123. R. Miller, Colloid & Polymer Sci., 259, 1124 (1981).

124. K.L. Sutherland, Austr. J. Sci. Res., A5, 683 (1952).

125. R.B. Bird, W.E. Stewart and E.N. Lightfoot, "Transport Phenomena," John Wiley & Sons Inc., New York (1960).

126. J. Lucassen, J. Chem. Soc. Faraday I, 72, 76 (1976).

127. G.D. Smith, "Numerical Solution of Partial Differential Equations: Finite Difference Method," Oxford University Press (2 nd ed.), Oxford (1978).

128. R. Miller, Colloids & Surfaces, 46, 75 (1990).

129. J.A. Kitchener and C.F. Cooper, Quart. Rev., 13, 71 (1959).

130. S. Ross and J.H. Bramfitt, J. Phys. Chem., 61, 1261 (1957).

131. M. Jansson, L. Eriksson and P. Skagerlind, Colloids and Surfaces, 53, 157 (1991).

132. S. Ross, J. Phys. Colloid Chem., 54, 429 (1950).

133. S. Ross and G.J. Young, Ind. Eng. Chem., 43, 2520 (1951).

134. S. Ross and G.D. Miles, Oil & Soaps, 18, 99 (1941).

135. T. Jiang, J. Chen and J.C. Slattery, J. Colloid Interface Sci., 96, 7 (1983).

136. D.T. Wasan, L. Gupta and M.K. Vora, J. AICHE, 17, 1287 (1971).

137. A.K. Chattopadhyay, L. Ghaicha, S.G. Oh and D.O. Shah, J. Phys. Chem., 96, 6509 (1992).

138. M. Jansson, A. Jonsson, P. Li and P. Stibs, Colloids and Surfaces, 59, 387 (1991).

139. A.G. Brown, W.C. Thurman and J.W. McBain, J. Colloid Sci., 8, 491 (1953).

140. A.G. Brown, W.C. Thurman and J.W. McBain, J. Colloid Sci., 8, 508 (1953).

141. Z. Yu and G. Xu, J. Phys. Chem., 93, 7441 (1989).

142. D.O. Shah, J. Colloid and Interface Sci., 32, 570 (1970).

143. D.O. Shah and C.A. Dysleski, J. Am. Oil Chem. Soc., 46, 645 (1970).

144. M.B. Stark, P. Skagerlind, K. Holmberg and J. Carlfors, Colloid & Polymer Sci., 268, 384 (1990).

145. P.D.I. Fletcher, R.B. Freeman, B.H. Robinson, G.D. Rees and R. Schomacker, Biochim. Biophys. Acta, 912, 278 (1987).

146. P.L. Lusi and L.J. Magid, CRC Crit. Rev. Biochem., 20, 409 (1986).

147. J.H. Fendler, "Membrane Mimetic Chemistry," John Wiley & Sons Inc., New York (1982), chapter 10.

148. D.G. Hayes and E. Gulari, Biotechnol. Bioeng., 35, 793 (1990).

149. K. Holmberg, J. Surface Sci. Technol., 5, 209 (1989).

150. A. Heisler, C. Rabiller and L. Hublin, Biotechnol. Lett., 13, 327 (1991).

151. S.M. Kim and J.S. Rhee, J. Am. Oil Chem. Soc., 68, 499 (1991).

152. K. Veeraragavan, Analytical Biochemistry, 186, 301 (1990).

153. R. Verger, M.C.E. Mieras and G.H. De Haas, J. Biol. Chem., 248, 4023 (1973).

154. F. Ergan, M. Trani and G. Andre, Biotechnol. Bioeng., 35, 195 (1990).

BIOGRAPHICAL SKETCH

Seong-Geun Oh was born on May 8, 1961, in the Republic of Korea. He received his B.S. degree in chemical engineering from Hanyang University in February, 1984. He joined the Korea Advanced Institute of Science and Technology in March, 1984, then received his M.S. degree through the study of colloid and interface science in 1986. From 1986 to 1989, he worked as a researcher in Pacific Chemical R & D Center. Specifically, he carried out much research about emulsion stability, biosurfactant and liquid crystal during this period.

Seong-Geun Oh received his Ph.D. in Chemical Engineering from the University of Florida under Professor D.O. Shah in 1993.

I certify that I have read this study and that in my opinion it conforms to acceptable standards of scholarly presentation and is fully adequate, in scope and quality, as a dissertation for the degree of Doctor of Philosophy.

Dinesh O. Shah, Chairman
Professor of Chemical Engineering

I certify that I have read this study and that in my opinion it conforms to acceptable standards of scholarly presentation and is fully adequate, in scope and quality, as a dissertation for the degree of Doctor of Philosophy.

Brij M. Moudgil
Professor of Materials Science and Engineering

I certify that I have read this study and that in my opinion it conforms to acceptable standards of scholarly presentation and is fully adequate, in scope and quality, as a dissertation for the degree of Doctor of Philosophy.

Ranganatha Narayanan
Professor of Chemical Engineering

I certify that I have read this study and that in my opinion it conforms to acceptable standards of scholarly presentation and is fully adequate, in scope and quality, as a dissertation for the degree of Doctor of Philosophy.

Chang Won Park
Associate Professor of Chemical Engineering

I certify that I have read this study and that in my opinion it conforms to acceptable standards of scholarly presentation and is fully adequate, in scope and quality, as a dissertation for the degree of Doctor of Philosophy.

Gerald B. Westermann-Clark
Associate Professor of Chemical Engineering

This dissertation was submitted to the Graduate Faculty of the College of Engineering and to the Graduate School and was accepted as partial fulfillment of the requirements for the degree of Doctor of Philosophy.

December, 1993

for Winfred M. Phillips
Dean, College of Engineering

Karen A. Holbrook
Dean, Graduate School